The ketone body β-hydroxybutyrate ameliorates neurodevelopmental deficits in the GABAergic system of *daf-18/PTEN Caenorhabditis elegans* mutants

Sebastián Giunti[1,2], María Gabriela Blanco[1,2], María José De Rosa[1,2*] and Diego Rayes[1,2*]

1-Instituto de Investigaciones Bioquímicas de Bahía Blanca (INIBIBB) CCT UNS-CONICET, Bahía Blanca, Argentina

2-Departamento de Biología, Bioquímica y Farmacia, Universidad Nacional Del Sur (UNS), Bahía Blanca, Argentina

Correspondence to:

Maria José De Rosa (mjderosa@criba.edu.ar)

Diego Rayes (drayes@criba.edu.ar)

Highlights

**daf-18/PTEN* deficiency in *C. elegans* results in a specific impairment of inhibitory GABAergic signaling, while the excitatory cholinergic signaling remains unaffected.

*The dysfunction of GABAergic neurons in these mutants arises from the inactivity of the transcription factor DAF-16/FOXO during their development, resulting in conspicuous morphological and functional alterations.

*A diet enriched with the ketone body β-hydroxybutyrate, which induces DAF-16/FOXO activity, mitigates the functional and morphological defects in the development of GABAergic neurons

*β-hydroxybutyrate supplementation during the early stages of development is both necessary and sufficient to achieve these rescuing effects on GABAergic signaling in *daf-18/PTEN* mutants.

Abstract

A finely tuned balance between excitation and inhibition (E/I) is essential for proper brain function. Disruptions in the GABAergic system, which alter this equilibrium, are a common feature in various types of neurological disorders, including Autism Spectrum Disorders (ASDs).

Mutations in PTEN, the main negative regulator of the PI3K/Akt pathway, are strongly associated with ASD. However, it is unclear whether PTEN deficiencies can differentially affect inhibitory and excitatory signaling. Using the *C. elegans* neuromuscular system, where both excitatory (cholinergic) and inhibitory (GABAergic) inputs regulate muscle activity, we found that *daf-18*/*PTEN* mutations specifically impact GABAergic (but not cholinergic) neurodevelopment and function. This selective impact results in a deficiency in inhibitory signaling. The specific defects observed in the GABAergic system in *daf-18/PTEN* mutants are due to reduced activity of DAF-16/FOXO during development. Ketogenic diets (KGDs) have proven effective for disorders associated with E/I imbalances. However, the mechanisms underlying their action remain largely elusive. We found that a diet enriched with the ketone body β-hydroxybutyrate during early development induces DAF-16/FOXO activity, therefore improving GABAergic neurodevelopment and function in *daf-18/PTEN* mutants. Our study provides valuable insights into the link between PTEN mutations and neurodevelopmental defects and delves into the mechanisms underlying the potential therapeutic effects of KGDs.

INTRODUCTION

Maintaining a delicate balance between excitatory and inhibitory (E/I) neurotransmission is critical for optimal brain function[1]. Disruptions in this balance are commonly observed in neurodevelopmental disorders[2-4]. In particular, deficits in inhibitory (GABAergic) signaling have been reported in Autism Spectrum Disorders (ASD) and other related physiopathological conditions[4,5].

PTEN is a classical tumor suppressor gene that antagonizes the highly conserved phosphatidylinositol 3-phosphate kinase (PI3K)/protein kinase B (PKB/Akt) pathway. Several reports using animal models have highlighted the importance of *PTEN* in neurodevelopment[6-12]. Moreover, mutations in *PTEN* were frequently found in human patients presenting ASD[13]. The molecular events underlying the neurodevelopmental deficits in *PTEN* mutants remain poorly understood.

The *C. elegans* neuromuscular system, where both excitatory (cholinergic) and inhibitory (GABAergic) motor neurons regulate muscle contraction and relaxation, provides an excellent platform for studying the function, balance, and coordination between excitatory and inhibitory signals[14-20]. This system has yielded valuable insights into fundamental synaptic transmission mechanisms[21,22]. Over the last decade, numerous studies focused on this simple yet highly informative system have significantly contributed to our understanding of the functioning and dysregulation of human genes associated with neurodevelopmental disorders, epilepsy, and familial hemiplegic migraine[14,19,20,23]. Furthermore, the substantial conservation of the main components of the PI3K/Akt pathway in *C. elegans*[24,25], enhances the applicability of this model system for investigating the role of this pathway in neurodevelopment.

We here found that mutations in *daf-18* (the ortholog for *PTEN* in *C. elegans*) result in specific impairments in GABAergic inhibitory signaling due to decreased activity of the transcription factor DAF-16 (the ortholog for FOXO in *C. elegans*) during neurodevelopment. Interestingly, cholinergic excitatory motor neurons remain unaffected. This targeted impairment of inhibitory signals causes

an imbalance between excitatory and inhibitory (E/I) neurotransmission in the animal's neuromuscular system.

In humans, ketogenic diets (KGDs), which force fatty acids beta-oxidation into ketone bodies, have been utilized for decades to treat pathologies associated with E/I imbalances, such as refractory epilepsies[26-28]. More recently, KGDs have also demonstrated effectiveness in alleviating autistic symptoms in humans[29] and rodent models of ASD[30,31]. The mechanisms underlying these beneficial effects remain largely unknown.

We demonstrated that exposing *daf-18/PTEN* mutants to a diet enriched with the ketone body β-hydroxybutyrate (βHB) early in development enhances DAF-16/FOXO activity, mitigates morphological and functional defects in GABAergic neurons, and improves behavioral phenotypes. This study not only provides a straightforward system for studying the role of the conserved PI3K/Akt/FOXO pathway in neurodevelopment but also contributes to our understanding of the mechanisms underlying the effects of ketone bodies in neurodevelopment.

RESULTS

Mutants in daf-18/PTEN and daf-16/FOXO are Hypersensitive to Cholinergic Drugs

Disturbances in *C. elegans* cholinergic or GABAergic activity can be detected by analyzing the sensitivity to the paralyzing effects of drugs that exacerbate cholinergic transmission[14,15]. We analyzed the sensitivity of *daf-18/PTEN* deficient animals to the acetylcholinesterase inhibitor aldicarb and the cholinergic agonist levamisole. Exposure to aldicarb leads to an increase in ACh levels at cholinergic motor synapses, resulting in massive activation of muscular cholinergic receptors and subsequent paralysis[32] (Figure 1A). Levamisole also induces paralysis by directly activating muscular cholinergic receptors[32] (Figure 1A). We found that *daf-18/PTEN* mutants are hypersensitive to the paralyzing effects of both drugs (Figures 1B and 1C). Hypersensitivity to cholinergic drugs is typical of animals with an increased E/I ratio in the neuromuscular system, such as mutants in *unc-25* (the *C. elegans* orthologue for glutamic acid decarboxylase, an

essential enzyme for synthesizing GABA)[14,15]. While *daf-18/PTEN* mutants become paralyzed earlier than wild-type animals, their hypersensitivity to cholinergic drugs is not as severe as that observed in animals completely deficient in GABA synthesis, such *unc-25* null mutants (Figures 1B and 1C) indicating a less pronounced imbalance between excitatory and inhibitory signals. Reduced activity of DAF-18/PTEN has been largely shown to exacerbate the PI3K pathway, precluding the activation of DAF-16/FOXO, the *C. elegans* ortholog of the FOXO transcription factors family[25] (Figure S1A). We analyzed aldicarb and levamisole sensitivity of mutants in this transcription factor. Similar to *daf-18/PTEN* mutants, we found that *daf-16/FOXO* null mutants are hypersensitive to the paralyzing effects of aldicarb and levamisole (Figure 1C). Furthermore, we did not observe significant differences in aldicarb and levamisole sensitivity between *daf-18; daf-16* double null mutants and the respective single mutants, suggesting that both genes affect neuromuscular signaling by acting in the same pathway (Figure 1C). In addition to *daf-16/FOXO* and *daf-18/PTEN*, we assessed the sensitivity to the paralyzing effects of aldicarb and levamisole in loss of function mutants of other components of the PI3K pathway, such as *age-1*/PI3K, *pdk-1, akt-1*, and *akt-2* (Figure 1D). Unlike mutations in *daf-18/PTEN*, in these mutants the PI3K pathway is downregulated (Figure S1A). We did not observe significant differences compared to the wild-type. Due to the complete dauer arrest observed in double mutants of *akt-1* and *akt-2*[33,34], we were unable to explore the potential redundancy of these two genes. Interestingly, a gain-of-function mutant in *pdk-1, pdk-1(mg142)*[24], is hypersensitive to aldicarb and levamisole, similar to *daf-16/FOXO* and *daf-18/PTEN* mutants (Figure 1D). Given that increased *pdk-1* activity is linked to hyperphosphorylation and inactivation of DAF-16/FOXO (Figure S1A), these results support the hypothesis that low activity of DAF-16/FOXO leads to hypersensitivity to these drugs.

In vertebrates, alterations in PTEN activity have been largely shown to impact neuronal development and function by affecting the mTOR pathway[35]. Consequently, we analyzed whether mutations in components of the *C. elegans* TOR complexes (TORC) would lead to significant changes in sensitivity to aldicarb and levamisole. Our findings indicate that neither animals with

loss of the essential TORC1 component *raga-1*/RagA nor animals with a loss of function in the essential TORC2 component *rict-1*/Rictor exhibited significant alterations in sensitivity to cholinergic drugs compared to wild-type animals (Figure 1E). This suggests that the mTOR pathway is not involved in *daf-18/PTEN* pharmacological phenotypes.

daf-18/PTEN and daf-16/FOXO Mutants Show Phenotypes Indicative of GABAergic Deficiency

In *C. elegans*, the body wall muscles receive cholinergic innervation, which induces contraction, and GABAergic innervation, which leads to relaxation. The contralateral activity of cholinergic and GABAergic neurons facilitates the characteristic undulatory movement of the animal (Figure 2A). Hypersensitivity to cholinergic drugs has long been observed in worms where GABAergic signaling is deficient[14,15] (Figure 1). In mutants with severe deficits in GABA transmission, prodding induces a bilateral contraction of the body wall muscles that shortens the body (shrinker phenotype)[36]. When *daf-18/PTEN* mutants are touched, there is a slight but significant shortening in body length (Figure 2B). As expected, this shortening is not as noticeable as in animals with a complete deficit in GABAergic signaling, such as mutants in *unc-25*. Similar to *daf-18/PTEN* mutants, *daf-16/FOXO* animals also exhibit a mild decrease in body length after prodding. Consistent with our aldicarb and levamisole results, there are no significant differences in body shortening between *daf-18;daf-16* double mutants and the corresponding single mutants (Figure 2B), further supporting the notion that both genes act in the same pathway to impact neuromuscular signaling.

We also analyzed other behaviors that require a concerted activity of GABAergic and cholinergic systems, such as the omega turns during the escape response[37]. In *C. elegans* the escape response can be induced by a gentle touch on the head and involves a backward movement that is usually followed by a sharp omega turn and a 180^{o} change in its direction of locomotion [37] (Movie 1). The execution of the omega turn involves a hypercontraction of the ventral muscles and relaxation of the dorsal muscles, allowing the animal to make a sharp turn, where the animal's

head slides on the ventral side of the body (closed omega turn), and resumes locomotion in the opposite direction (Movie 1). In response to anterior touch, the vast majority of wild-type worms make a closed omega turn[37,38](Figure 2C). Ventral muscle contraction is triggered by cholinergic motor neurons (VA and VB neurons) that synapse onto ventral muscles, while dorsal muscle relaxation is induced by GABAergic motor neurons (DD neurons) that synapse onto dorsal muscles (Figure 2A)[37,38]. Ablation of DD GABAergic neurons reduces dorsal muscle relaxation, therefore preventing the head from touching the ventral side of the body during the escape response (open omega turn)[37]. In agreement with previous reports, we found that 91% of wild-type animals exert a closed omega turn within the escape response (Figure 2C). We observed that similar to wild-type animals, gentle anterior touch with an eyelash induces *daf-18* mutants to move backward and initiate an omega turn (Movie 2). However, only 53% of *daf-18* mutants exhibit the typical head-to-tail contact during the omega turn (Figure 2C and Movie 2). Akin to *daf-18* mutants, *daf-16/FOXO* mutants exhibited a decrease in the proportion of closed omega turns (Figure 2C). No additive effects were observed in the *daf-18; daf-16* double mutant, suggesting that the increased inactivation of *daf-16/FOXO* is primarily responsible for the defects observed in the escape response of *daf-18* mutants.

Given that our results suggest a deficit in GABAergic functionality in *daf-18/PTEN* mutants, we used optogenetics to specifically activate these neurons in mutant worms. The expression of Channelrhodopsin (ChR2) in GABAergic motor neurons (using the *unc-47* promoter, orthologue for the vesicular GABA transporter SLC32A1) elicits a flaccid paralysis of the worms upon exposure to blue light. This obvious and robust response results in an increase in body length that can be used as a clear readout[39-41](Figure 2D and Movie 3). Interestingly, we found that the elongation of the animal after the specific activation of GABAergic neurons is significantly decreased in *daf-18/PTEN* and *daf-16/FOXO* mutants compared to wild-type worms (Figure 2D). While these results suggest a defect in GABAergic transmission, it could also be possible that general neuronal transmission is affected. Consequently, we reciprocally activated the cholinergic

motor neurons in animals expressing ChR2 under the *unc-17* promoter, a gene encodes the vesicular acetylcholine transporter (VAChT), which leads to muscle contraction and shortened body length[39,41](Figure 2E and Movie 4). Rather than observing reduced shortening in *daf-16/FOXO* and *daf-18/PTEN* mutants, we found that cholinergic activation caused hypercontraction of these mutant animals (Figure 2E). Since the activation of cholinergic motor neurons not only activates muscles but also stimulates GABAergic neurons to produce counteractive muscle relaxation in the other side of the animal (Figure 2A), it is expected that a GABAergic deficit would lead to increased muscle contraction and body shortening upon cholinergic activation. In summary, these results strongly suggest that in *daf-18/PTEN* and *daf-16/FOXO* mutants, there is a specific functional defect in GABAergic neurons, while excitatory neurons do not appear to be affected.

Disruption of daf-18/PTEN Alters Commissural Trajectories in GABAergic Motor Neurons

Since our previous results imply perturbations of neuromuscular transmission, we explored the morphology of *C. elegans* motor neurons. The cell bodies of both cholinergic (A and B-type) and GABAergic (D-type) motor neurons that innervate body wall muscles are located in the ventral nerve cord (VNC), and a subset extends single process commissures to the dorsal nerve cord (DNC) [42] (Figures 3A and S2). The commissures have proved useful for studying defects in motor neuron development or maintenance[43,44]. We analyzed the morphology of GABAergic motor neurons in L4 animals expressing *mCherry* under the control of the *unc-47* promoter[45]. We found that *daf-18/PTEN* mutants exhibit a higher frequency of commissure flaws, including guidance defects, ectopic branching, and commissures that fail to reach the dorsal cord (Figures 3B and 3C). In contrast to our findings in GABAergic neurons, we observed no obvious differences in the frequency of commissure defects when we compared cholinergic motor neurons in control and *daf-18/PTEN* animals (Figure S2).

GABAergic motor neurons can be classified based on the muscles they innervate: those that innervate the dorsal muscles are called DDs, while those that innervate the ventral muscles are called VDs. Both types of D neurons send commissures to the DNC[46,47]. We found defects in various commissures, some of which correspond to VD and others to DD neurons (Figure S3). We also analyzed GABAergic commissures at the beginning (1 hour post-hatching) of the first larval stage (L1), when only the six DD neurons are formed[46,48,49]. We found that in this early larval stage, *daf-18/PTEN* mutants exhibit defects in the GABAergic commissures (Figures 3D, 3E and S4). While the DD neurons are born and mostly develop embryonically, limited postembryonic axonal outgrowth has been observed in these neurons[49]. We did not find an increase in the number of errors in larvae 5-6 hours post-hatching compared to recently hatched larvae (Figure S4B), indicating that deficiencies in DD neurons in *daf-18/PTEN* mutants mainly occur during their embryonic development. In contrast, we observed that the prevalence of errors increases significantly at the L4 stage (Figure S4B and S4C). The greater number of defects in L4s likely arises from defects in the VDs, which are born post-embryonically between the mid-L1 larval stage and the L2 stage, and add to the defects already present in the DDs. Taken together, these observations suggest that reduced DAF-18/PTEN activity affects the neurodevelopment of the GABAergic motor system. Since the transcription factor DAF-16/FOXO is one of the main targets of DAF-18/PTEN signaling, we analyzed the morphology of GABAergic motor neurons in *daf-16/FOXO* null mutants. These animals also exhibit an increased number of defects in GABAergic commissures compared to the wild type (Figure 3C).

Given that *daf-18* is ubiquitously expressed in all tissues[25], we asked whether DAF-18/PTEN acts autonomously in GABAergic neurons to ensure proper development. We found that specific *daf-18/PTEN* expression in GABAergic neurons increased the proportion of closed omega turns in *daf-18/PTEN* null mutants (Figure 3F). In addition, the morphological defects in GABAergic commissures were significantly reduced (Figure 3G), suggesting that DAF-18/PTEN acts autonomously in GABAergic motor neurons to regulate their development.

Collectively, our findings demonstrate that mutations in *daf-18/PTEN* and *daf-16/FOXO* result in developmental defects in GABAergic neurons, leading to both altered morphology and function, while leaving cholinergic motor neurons unaffected. Our experiments strongly suggest that these specific defects in the inhibitory transmission arise from the hyperactivation of the PI3K pathway, along with subsequent DAF-16/FOXO inhibition, in GABAergic neurons of *daf-18/PTEN* mutants.

A diet enriched with the ketone body β-hydroxybutyrate (βHB) Ameliorates Defects in daf18/PTEN Mutants but not in daf-16/FOXO Mutants

Mutations in *PTEN* are linked with Autism Spectrum Disorders (ASD)[6]. Ketogenic diets, which force the endogenous production of KBs, have proved to be effective for the treatment of neurological disorders associated with E/I imbalances, such as epilepsy and, more recently, ASD [27-29]. It has been shown that the KB βHB induces DAF-16/FOXO activity[50]. Therefore, we asked whether it is possible to improve the observed phenotypes by modulating the activity of DAF-16/FOXO with βHB. We first evaluated the expression of *sod-3*, which codes for a superoxide dismutase and is a DAF-16/FOXO transcriptional target gene[51]. We used a strain expressing a GFP transcriptional reporter for *sod-3* and determined fluorescence intensity upon dietary supplementation of βHB. Consistent with previous reports, the levels of SOD-3::GFP are reduced in *daf-18/PTEN* and *daf-16/FOXO* mutant strains. Furthermore, we observed that βHB (20 mM) induces the expression of *sod-3* in *daf-18/PTEN* but not in *daf-16/FOXO* mutants (Figure S5). Importantly, we did not detect increased *sod-3* expression in *daf-18; daf-16* double deficient animals, strongly suggesting that βHB induces *sod-3* expression in *daf-18/PTEN* mutants through the transcription factor *daf-16/FOXO* (Figure S5).

Next, we evaluated behavioral phenotypes and GABAergic neuronal morphology of animals that were raised on an *E. coli* diet supplemented with 20 mM βHB throughout development, from egg laying until the time of the assay (typically late L4s or young adults). We found that βHB supplementation significantly reduced the hypersensitivity of *daf-18/PTEN* mutants to the

cholinergic drugs aldicarb and levamisole (Figures 4A and 4B). Moreover, βHB supplementation rescued the post-prodding shortening in *daf-18/PTEN* mutants (Figure 4C). Accordingly, we found that *daf-18/PTEN* mutants showed a significant increase in the proportion of closed omega turns during their escape response compared to the naïve condition (Figure 4D). In contrast, βHB exposure does not change the number of closed omega turns in *daf-16/FOXO* null mutants or the double null mutant *daf-18; daf-16* (Figure 4D).

We subsequently analyzed the changes in body length induced by optogenetic activation of both GABAergic and cholinergic neurons in animals exposed to a diet enriched with βHB. Interestingly, we found that *daf-18/PTEN* mutants exposed to βHB, but not wild-type or *daf-16/FOXO* mutant animals, exhibited increased elongation following optogenetic activation of GABAergic neurons (Figures 4E, 4F, and 4G). Furthermore, we observed that the hypercontraction observed in *daf-18/PTEN* mutants after the activation of cholinergic neurons is significantly reduced in animals exposed to βHB (Figures 4H, 4I and 4J). These findings suggest that this ketone body can rebalance excitatory and inhibitory signals in the neuromuscular system of *daf-18/PTEN C. elegans* mutants.

We also evaluated the morphology of GABAergic motor neurons in *daf-18/PTEN* animals exposed to βHB. We found that βHB supplementation reduced the frequency of defects in GABAergic processes (Figure 4K). Consistently, βHB exposure did not significantly reduce the defects on GABAergic neurons of either *daf-16/FOXO* null mutants or *daf-18; daf-16* double mutants. Taken together, these results demonstrate that dietary βHB ameliorates the defects associated with deficient GABAergic signaling in *daf-18/PTEN* mutants.

It is noteworthy that we did not observe any improvement in either neuronal outgrowth defects in the AIY interneuron or the migration of the HSN motor neurons (Figure S6) in *daf-18/PTEN* mutants exposed to βHB, even though these defects were shown to depend on the reduction of DAF-16/FOXO activity [52,53]. AIY neurite and HSN soma migration take place during

254 embryogenesis [52,54]. It is therefore possible that βHB may not go through the impermeable chitin
255 eggshell of the embryo, as has been reported with other drugs (see below) [55].
256
257 *β-Hydroxybutyrate Exposure During Early L1 Development Sufficiently Mitigates GABAergic*
258 *System Defects*
259 In the above experiments, animals were exposed to βHB throughout development. We next asked
260 whether there is a critical period during development where the action of βHB is required. We
261 exposed *daf-18/PTEN* mutant animals to βHB-supplemented diets for 18-hour periods at different
262 developmental stages (Figure 5A). The earliest exposure occurred during the 18 hours following
263 egg laying, covering *ex-utero* embryonic development and the first 8-9 hours of the L1 stage. The
264 second exposure period encompassed the latter part of the L1 stage, the entire L2 stage, and
265 most of the L3 stage. The third exposure spanned the latter part of the L3 stage, the entire L4
266 stage, and the first 6-7 hours of the adult stage (Figure 5A). Interestingly, we found that the earliest
267 exposure to βHB was sufficient to increase the proportion of *daf-18/PTEN* mutant animals
268 executing a closed omega turn during the escape response. However, when the animals were
269 exposed to βHB at later juvenile stages, their ability to enhance the escape response of *daf-*
270 *18/PTEN* mutants declined (Figure 5B). Moreover, exposing animals to βHB for 18 hours starting
271 from egg laying was enough to reduce morphological defects in the GABAergic motor neurons of
272 these mutants (Figure 5C and Figure S7). Interestingly, βHB has no effect on GABAergic
273 commissures in either recently hatched L1s or L4 *daf-18/PTEN* mutants when exposure is limited
274 to the first 9 hours after egg laying (where *ex utero* embryonic development occurs), possibly due
275 to the impermeability of the chitinous eggshell (Figure S7). Thus, it is likely that βHB acts at early
276 L1 stages to mitigate neurological GABAergic defects in *daf-18/PTEN* mutants.
277 Taken together, our findings demonstrate that mutations in *daf-18*, the *C. elegans* orthologue of
278 PTEN, lead to specific defects in inhibitory GABAergic neurodevelopment without significantly
279 affecting cholinergic excitatory signals. These GABA-specific deficiencies manifest as altered

neuronal morphology, hypersensitivity to cholinergic stimulation, reduced responses to optogenetic GABAergic neuronal activation, mild body shortening following touch stimuli, and deficits in the execution of the omega turn. We have determined that these impairments in GABAergic development result from reduced activity of the FOXO orthologue DAF-16 in *daf-18/PTEN* mutants. Importantly, our study's pivotal finding is that a βHB- enriched diet during early development, robustly mitigates the deleterious effects of *daf-18/PTEN* mutations in GABAergic neurons. This protective effect is critically dependent on the induction of DAF-16/FOXO by this ketone body.

DISCUSSION

Mutations in *daf-18/PTEN* are linked to neurodevelopmental defects from worms to mammals[11,52,53]. Moreover, decreased activity of PTEN produces E/I disequilibrium and the development of seizures in mice [7]. The mechanisms underlying this imbalance are not clear. Our results demonstrate that reduced DAF-18/PTEN activity in *C. elegans* generates guidance defects, abnormal branching, incomplete commissural outgrowth and deficient function of inhibitory GABAergic neurons, without affecting the excitatory cholinergic neurons.

daf-18/PTEN deficient mutants have a shorter lifespan[56]. One possibility is that the defects in GABAergic processes are due to neurodegeneration associated with premature aging rather than developmental flaws. However, this idea is unlikely given that the neuronal defects in DD neurons are already evident at the early L1 stage. In *C. elegans*, DD GABAergic motor neurons undergo rearrangements during the L1-L2 stages[48,49]. In newly hatched L1 larvae, each DD motor neuron innervates ventral muscles and extends a commissure to the dorsal nerve cord to receive synaptic inputs from cholinergic DA and DB neurons[48,49,57]. In adults, the DD commissure morphology is maintained, but the synaptic output shifts to dorsal muscles, and input is provided by VA and VB cholinergic motor neurons in the ventral nerve cord[57]. A plausible possibility is that this remodeling process makes DD neurons specifically sensitive to PI3K pathway activity. However, since the

DD commissures are defective already at the very early L1 stage (prior to rewiring) and similar defects are observed in VD neurons, which are born post-embryonically between late L1 and L2 stages and do not undergo this remodeling[46,49,57], we can infer that the deficits caused by *daf-18/PTEN* deficiency affect the development of the entire GABAergic system, independently of the synaptic rearrangement of DD neurons.

Strikingly, cholinergic neurons have no noticeable morphological or functional defects in *daf-18/PTEN* mutants. Loss-of-function mutants in the neuronal integrin *ina-1,* ortholog of human ITGA6, affect the guidance of GABAergic commissures, without affecting cholinergic neurons [44]. Similar to *PTEN*, mutations in neuronal integrins have been linked to neurodevelopmental defects [58]. Interestingly, the PI3K/Akt/FOXO pathway and integrin signaling are interrelated in mammals [59]. This observation opens the possibility that one of the mechanisms by which *daf-18/PTEN* mutants have defects in GABAergic neurodevelopment involves integrin expression and/or function. Interestingly, mutations in *eel-1*, the *C. elegans* ortholog of HUWE1, or in subunits of the Anaphase-Promoting Complex (APC), lead to developmental and functional alterations in GABAergic neurons but not in cholinergic neurons[19,60], despite their expression in both neuronal types. This observation suggests the existence of compensatory or redundant mechanisms in cholinergic neurons that may not be present in GABAergic neurons.

In mammals, defects in *PTEN* mutants have been typically related to altered function of the mTOR pathway[8,61,62]. However, our results suggest that, in the *C. elegans* neuromuscular system, decreased activity of DAF-18/PTEN affects GABAergic development due to a downregulation of DAF-16/FOXO transcription factor activity. The FOXO family of transcription factors is conserved throughout the animal kingdom[63]. There is increasing evidence demonstrating the key role of this transcription factors family in neurodevelopment[64-66]. Downregulation of FOXO activity early in development reproduces neuropathological features found in ASD patients, i.e., increased brain size and cortical thickness[67,68]. The autonomic activity of DAF-18/PTEN and DAF-16/FOXO coordinates axonal outgrowth in *C. elegans* AIY interneurons and rat cerebellar granule neurons

[52]. On the other hand, DAF-18/PTEN and DAF-16/FOXO in the hypodermis control neuronal migration of the HSN neuron during development[53]. Our rescue experiments strongly suggest that the PI3K/Akt/DAF-16 pathway modulates the development of GABAergic motor neurons by acting autonomously in these cells. Noteworthy, autonomic DAF-16/FOXO activity in GABAergic motor neurons is also key for axonal growth during regeneration[69]. These results further emphasize the importance of DAF-16/FOXO in neuronal development and axonal growth.

In many patients suffering from epilepsy, ketogenic diets can control seizures[27,28]. Furthermore, they can reduce behavioral abnormalities in individuals with ASD[29]. While the mechanisms underlying the clinical effects of ketogenic diets remain unclear, it has been shown that these diets correlate with increased GABA signaling[70-72]. We demonstrate here that dietary supplementation of the ketone body βHB ameliorates morphological and functional defects in GABAergic motor neurons of *daf-18/PTEN* mutants. Although ketone bodies were historically viewed as simple carriers of energy to peripheral tissues during prolonged fasting or exercise, our findings confirm more recent reports showing that βHB also possesses a variety of important signaling functions[73]. We can hypothesize several distinct, non-mutually exclusive models by which βHB can induce DAF-16/FOXO-dependent signaling. βHB directly inhibits mammalian histone deacetylases HDAC1 and HDAC2, increasing histone acetylation at the FOXO3a promoter and inducing the expression of this gene[74]. HDAC1 and HDAC2 play an important role as redundant regulators of neuronal development[75]. Interestingly, in *C. elegans* βHB inhibits the class I HDACs to extend worm lifespan in a DAF-16/FOXO-dependent manner[50]. Therefore, βHB-mediated HDAC inhibition may upregulate transcription of DAF-16/FOXO counterbalancing hyperactivation of the PI3K pathway in *daf-18/PTEN* mutants. Another potential mechanism for the effect of βHB involves the inhibition of the insulin signaling pathway. In mammals, the administration of βHB downregulates the insulin signaling in muscle[76]. Moreover, several reports have shown that βHB administration reduces phosphorylation and activity of Akt/protein kinase downstream of the insulin receptor [77,78]. In *C. elegans*, inhibition of AKT-1 activates DAF-16/FOXO

[79]. Although understanding the mechanism behind βHB's action will require further studies, our results demonstrate that this ketone body positively modulates DAF-16/FOXO during neuronal development.

Multiple reports, from *C. elegans* to mammals, suggest that there is a sensitive period, typically early in development, where pharmacological or genetic interventions are more effective in ameliorating the consequences of neurodevelopmental defects[80]. However, recent evidence shows that phenotypes associated with certain neurodevelopmental defects can be ameliorated by interventions during adulthood[81]. Our results show that βHB can ameliorate the phenotypic defects of *daf-18/PTEN* mutants only when exposure occurs during an early critical period. The inefficacy of βHB at later stages suggests that the role of DAF-16/FOXO in the maintenance of GABAergic neurons is not as relevant as its role in development.

Our experiments do not allow us to distinguish whether the effect of βHB is preventive, reversive, or both. Our results suggest that the improvement is not due to prevention in DDs because the defects are present in newly hatched larvae regardless of the presence or absence of βHB, and DD post-embryonic growth does not add new errors. Unlike in early L1 stages, the protective effect of βHB becomes evident when analyzing the commissures of L4 animals. In this late larval stage, not only the DDs but also the VD neurons are present. This leads us to speculate that βHB may have a preventive action on the neurodevelopment of VD neurons. We also cannot rule out that this improvement may be due, at least partially, to a reversal of defects in DD neurons. It is intriguing how exposure to βHB during early L1 could ameliorate defects in neurons that mainly emerge in late L1s (VDs). We can hypothesize that residual βHB or a metabolite from the previous exposure may prevent these defects in VD neurons. βHB, in particular, has been shown to generate long-lasting effects through epigenetic modifications[82]. Further investigations are needed to elucidate the underlying fundamental mechanisms regarding the ameliorating effects of βHB supplementation on deficits in GABAergic neurodevelopment associated with mutations in *daf-18/PTEN*.

Across the animal kingdom, food signals increase insulin levels leading to the activation of Akt/PI3K pathway[83-85]. In *C. elegans*, the L1 larval stage is particularly sensitive to nutritional status. *C. elegans* adjusts its development based on food availability, potentially arresting in L1 in the absence of food[86]. Strong loss-of-function alleles in the insulin signaling pathway exhibit constitutive L1 arrest[87], highlighting the critical importance of this pathway during this larval stage. Hence, it is not surprising that dietary interventions targeting the PI3K pathway at these critical early L1 stages can modulate developmental processes. Our pharmacological experiments showed that mutants associated with an exacerbation of the PI3K pathway, which typically inhibits the nuclear translocation and activity of the transcription factor DAF-16/FOXO, lead to E/I imbalances that manifest as hypersensitivity to cholinergic drugs. We demonstrated that these imbalances arise from defects that occur specifically in the neurodevelopment of GABAergic motor neurons. Interestingly, mutants inhibiting the PI3K pathway do not show differences in their sensitivity to cholinergic drugs compared to wild-type animals. This observation can be explained by a critical period during neurodevelopment when the Insulin/Akt/PI3K pathway must be maintained at very low activity (or even deactivated). These low activity levels of the Insulin/Akt/PI3K pathway would allow for a high level of DAF-16/FOXO activity, which, according to our results, appears to be key for the proper development of GABAergic neurons.

The fine regulation of insulin and insulin-like signaling during early development is a conserved process in animals[88,89]. In mammals, for instance, conditions like Gestational Diabetes Mellitus (GDM), characterized by fetal hyperinsulinemia and high levels of IGF-1[90], are associated with neurodevelopmental defects[91]. Our results lead to the intriguing idea that dietary interventions that increase DAF-16/FOXO activity, such as βHB supplementation, could constitute a potential therapeutic strategy for these pathologies. Future studies using mammalian models are crucial to shed light on the potential of this hypothesis.

References

1 Tao, H. W., Li, Y. T. & Zhang, L. I. Formation of excitation-inhibition balance: inhibition listens and changes its tune. *Trends Neurosci* **37**, 528-530, doi:10.1016/j.tins.2014.09.001 (2014).

2 Bozzi, Y., Provenzano, G. & Casarosa, S. Neurobiological bases of autism-epilepsy comorbidity: a focus on excitation/inhibition imbalance. *Eur J Neurosci* **47**, 534-548, doi:10.1111/ejn.13595 (2018).

3 Coghlan, S. *et al.* GABA system dysfunction in autism and related disorders: from synapse to symptoms. *Neurosci Biobehav Rev* **36**, 2044-2055, doi:10.1016/j.neubiorev.2012.07.005 (2012).

4 Oblak, A., Gibbs, T. T. & Blatt, G. J. Decreased GABAA receptors and benzodiazepine binding sites in the anterior cingulate cortex in autism. *Autism Res* **2**, 205-219, doi:10.1002/aur.88 (2009).

5 Gogolla, N. *et al.* Common circuit defect of excitatory-inhibitory balance in mouse models of autism. *J Neurodev Disord* **1**, 172-181, doi:10.1007/s11689-009-9023-x (2009).

6 Rademacher, S. & Eickholt, B. J. PTEN in Autism and Neurodevelopmental Disorders. *Cold Spring Harb Perspect Med* **9**, doi:10.1101/cshperspect.a036780 (2019).

7 van Diepen, M. T. & Eickholt, B. J. Function of PTEN during the formation and maintenance of neuronal circuits in the brain. *Developmental neuroscience* **30**, 59-64, doi:10.1159/000109852 (2008).

8 Kwon, C. H. *et al.* Pten regulates neuronal arborization and social interaction in mice. *Neuron* **50**, 377-388, doi:10.1016/j.neuron.2006.03.023 (2006).

9 Smith, G. D., White, J. & Lugo, J. N. Superimposing Status Epilepticus on Neuron Subset-Specific PTEN Haploinsufficient and Wild Type Mice Results in Long-term Changes in Behavior. *Sci Rep* **6**, 36559, doi:10.1038/srep36559 (2016).

10 Clipperton-Allen, A. E. & Page, D. T. Pten haploinsufficient mice show broad brain overgrowth but selective impairments in autism-relevant behavioral tests. *Hum Mol Genet* **23**, 3490-3505, doi:10.1093/hmg/ddu057 (2014).

11 Chen, Y., Huang, W. C., Sejourne, J., Clipperton-Allen, A. E. & Page, D. T. Pten Mutations Alter Brain Growth Trajectory and Allocation of Cell Types through Elevated beta-Catenin Signaling. *J Neurosci* **35**, 10252-10267, doi:10.1523/JNEUROSCI.5272-14.2015 (2015).

12 Clipperton-Allen, A. E. *et al.* Pten haploinsufficiency causes desynchronized growth of brain areas involved in sensory processing. *iScience* **25**, 103796, doi:10.1016/j.isci.2022.103796 (2022).

13 Butler, M. G. *et al.* Subset of individuals with autism spectrum disorders and extreme macrocephaly associated with germline PTEN tumour suppressor gene mutations. *J Med Genet* **42**, 318-321, doi:10.1136/jmg.2004.024646 (2005).

14 Huang, Y. C. *et al.* Gain-of-function mutations in the UNC-2/CaV2alpha channel lead to excitation-dominant synaptic transmission in Caenorhabditis elegans. *Elife* **8**, doi:10.7554/eLife.45905 (2019).

15 Vashlishan, A. B. *et al.* An RNAi screen identifies genes that regulate GABA synapses. *Neuron* **58**, 346-361, doi:10.1016/j.neuron.2008.02.019 (2008).

16 Zhou, X. & Bessereau, J. L. Molecular Architecture of Genetically-Tractable GABA Synapses in C. elegans. *Front Mol Neurosci* **12**, 304, doi:10.3389/fnmol.2019.00304 (2019).

17 Safdie, G. *et al.* RIC-3 phosphorylation enables dual regulation of excitation and inhibition of Caenorhabditis elegans muscle. *Mol Biol Cell* **27**, 2994-3003, doi:10.1091/mbc.E16-05-0265 (2016).

18 Stawicki, T. M., Zhou, K., Yochem, J., Chen, L. & Jin, Y. TRPM channels modulate epileptic-like convulsions via systemic ion homeostasis. *Current biology : CB* **21**, 883-888, doi:10.1016/j.cub.2011.03.070 (2011).

19 Opperman, K. J. *et al.* The HECT Family Ubiquitin Ligase EEL-1 Regulates Neuronal Function and Development. *Cell Rep* **19**, 822-835, doi:10.1016/j.celrep.2017.04.003 (2017).

20 Giles, A. C. *et al.* A complex containing the O-GlcNAc transferase OGT-1 and the ubiquitin ligase EEL-1 regulates GABA neuron function. *The Journal of biological chemistry* **294**, 6843-6856, doi:10.1074/jbc.RA119.007406 (2019).

21 Blazie, S. M. & Jin, Y. Pharming for Genes in Neurotransmission: Combining Chemical and Genetic Approaches in Caenorhabditis elegans. *ACS Chem Neurosci* **9**, 1963-1974, doi:10.1021/acschemneuro.7b00509 (2018).

22 Calahorro, F. & Izquierdo, P. G. The presynaptic machinery at the synapse of C. elegans. *Invertebrate neuroscience : IN* **18**, 4, doi:10.1007/s10158-018-0207-5 (2018).

23 Bessa, C., Maciel, P. & Rodrigues, A. J. Using C. elegans to decipher the cellular and molecular mechanisms underlying neurodevelopmental disorders. *Molecular neurobiology* **48**, 465-489, doi:10.1007/s12035-013-8434-6 (2013).

24 Paradis, S. & Ruvkun, G. Caenorhabditis elegans Akt/PKB transduces insulin receptor-like signals from AGE-1 PI3 kinase to the DAF-16 transcription factor. *Genes Dev* **12**, 2488-2498, doi:10.1101/gad.12.16.2488 (1998).

25 Ogg, S. & Ruvkun, G. The C. elegans PTEN homolog, DAF-18, acts in the insulin receptor-like metabolic signaling pathway. *Molecular cell* **2**, 887-893, doi:10.1016/s1097-2765(00)80303-2 (1998).

26 D'Andrea Meira, I. *et al.* Ketogenic Diet and Epilepsy: What We Know So Far. *Front Neurosci* **13**, 5, doi:10.3389/fnins.2019.00005 (2019).

27 Neal, E. G. *et al.* The ketogenic diet for the treatment of childhood epilepsy: a randomised controlled trial. *The Lancet. Neurology* **7**, 500-506, doi:10.1016/S1474-4422(08)70092-9 (2008).

28 Lambrechts, D. A. *et al.* A randomized controlled trial of the ketogenic diet in refractory childhood epilepsy. *Acta Neurol Scand* **135**, 231-239, doi:10.1111/ane.12592 (2017).

29 Li, Q., Liang, J., Fu, N., Han, Y. & Qin, J. A Ketogenic Diet and the Treatment of Autism Spectrum Disorder. *Frontiers in pediatrics* **9**, 650624, doi:10.3389/fped.2021.650624 (2021).

30 Castro, K., Baronio, D., Perry, I. S., Riesgo, R. D. S. & Gottfried, C. The effect of ketogenic diet in an animal model of autism induced by prenatal exposure to valproic acid. *Nutritional neuroscience* **20**, 343-350, doi:10.1080/1028415X.2015.1133029 (2017).

31 Verpeut, J. L., DiCicco-Bloom, E. & Bello, N. T. Ketogenic diet exposure during the juvenile period increases social behaviors and forebrain neural activation in adult Engrailed 2 null mice. *Physiol Behav* **161**, 90-98, doi:10.1016/j.physbeh.2016.04.001 (2016).

32 Mahoney, T. R., Luo, S. & Nonet, M. L. Analysis of synaptic transmission in Caenorhabditis elegans using an aldicarb-sensitivity assay. *Nature protocols* **1**, 1772-1777, doi:10.1038/nprot.2006.281 (2006).

33 Oh, S. W. *et al.* JNK regulates lifespan in Caenorhabditis elegans by modulating nuclear translocation of forkhead transcription factor/DAF-16. *Proc Natl Acad Sci U S A* **102**, 4494-4499, doi:10.1073/pnas.0500749102 (2005).

34 Quevedo, C., Kaplan, D. R. & Derry, W. B. AKT-1 regulates DNA-damage-induced germline apoptosis in C. elegans. *Current biology : CB* **17**, 286-292, doi:10.1016/j.cub.2006.12.038 (2007).

35 Skelton, P. D., Stan, R. V. & Luikart, B. W. The Role of PTEN in Neurodevelopment. *Mol Neuropsychiatry* **5**, 60-71, doi:10.1159/000504782 (2020).

36 McIntire, S. L., Jorgensen, E., Kaplan, J. & Horvitz, H. R. The GABAergic nervous system of Caenorhabditis elegans. *Nature* **364**, 337-341, doi:10.1038/364337a0 [doi] (1993).

37 Donnelly, J. L. *et al.* Monoaminergic orchestration of motor programs in a complex C. elegans behavior. *PLoS. Biol* **11**, e1001529, doi:10.1371/journal.pbio.1001529 [doi];PBIOLOGY-D-12-03108 [pii] (2013).

38 Pirri, J. K. & Alkema, M. J. The neuroethology of C. elegans escape. *Curr. Opin. Neurobiol* **22**, 187-193, doi:S0959-4388(11)00225-X [pii];10.1016/j.conb.2011.12.007 [doi] (2012).

39 Hwang, H. *et al.* Muscle contraction phenotypic analysis enabled by optogenetics reveals functional relationships of sarcomere components in Caenorhabditis elegans. *Sci Rep* **6**, 19900, doi:10.1038/srep19900 (2016).

40 Schultheis, C., Brauner, M., Liewald, J. F. & Gottschalk, A. Optogenetic analysis of GABAB receptor signaling in Caenorhabditis elegans motor neurons. *J Neurophysiol* **106**, 817-827, doi:10.1152/jn.00578.2010 (2011).

41 Koopman, M., Janssen, L. & Nollen, E. A. A. An economical and highly adaptable optogenetics system for individual and population-level manipulation of Caenorhabditis elegans. *BMC Biol* **19**, 170, doi:10.1186/s12915-021-01085-2 (2021).

42 Altun, Z. & Hall, D. Nervous system, general description. *WormAtlas. doi* **10**, 103-116 (2011).

43 Cáceres Ide, C., Valmas, N., Hilliard, M. A. & Lu, H. Laterally orienting C. elegans using geometry at microscale for high-throughput visual screens in neurodegeneration and neuronal development studies. *PLoS One* **7**, e35037, doi:10.1371/journal.pone.0035037 (2012).

44 Oliver, D. *et al.* Integrins Have Cell-Type-Specific Roles in the Development of Motor Neuron Connectivity. *J Dev Biol* **7**, doi:10.3390/jdb7030017 (2019).

45 Byrne, A. B. *et al.* Inhibiting poly(ADP-ribosylation) improves axon regeneration. *Elife* **5**, doi:10.7554/eLife.12734 (2016).

46 Sulston, J. E. & White, J. G. Regulation and cell autonomy during postembryonic development of Caenorhabditis elegans. *Developmental biology* **78**, 577-597, doi:10.1016/0012-1606(80)90353-x (1980).

47 White, J. G., Southgate, E., Thomson, J. N. & Brenner, S. The structure of the nervous system of the nematode Caenorhabditis elegans. *Philos. Trans. R. Soc. Lond B Biol. Sci* **314**, 1-340 (1986).

48 Hallam, S. J. & Jin, Y. lin-14 regulates the timing of synaptic remodelling in Caenorhabditis elegans. *Nature* **395**, 78-82, doi:10.1038/25757 (1998).

49 Mulcahy, B. *et al.* Post-embryonic remodeling of the C. elegans motor circuit. *Current biology : CB* **32**, 4645-4659 e4643, doi:10.1016/j.cub.2022.09.065 (2022).

50 Edwards, C. *et al.* D-beta-hydroxybutyrate extends lifespan in C. elegans. *Aging* **6**, 621-644, doi:10.18632/aging.100683 (2014).

51 De Rosa, M. J. *et al.* The flight response impairs cytoprotective mechanisms by activating the insulin pathway. *Nature* **573**, 135-138, doi:10.1038/s41586-019-1524-5 (2019).

52 Christensen, R., de la Torre-Ubieta, L., Bonni, A. & Colon-Ramos, D. A. A conserved PTEN/FOXO pathway regulates neuronal morphology during C. elegans development. *Development* **138**, 5257-5267, doi:10.1242/dev.069062 (2011).

53 Kennedy, L. M., Pham, S. C. & Grishok, A. Nonautonomous regulation of neuronal migration by insulin signaling, DAF-16/FOXO, and PAK-1. *Cell Rep* **4**, 996-1009, doi:10.1016/j.celrep.2013.07.045 (2013).

54 Hedgecock, E. M., Culotti, J. G., Hall, D. H. & Stern, B. D. Genetics of cell and axon migrations in Caenorhabditis elegans. *Development* **100**, 365-382, doi:10.1242/dev.100.3.365 (1987).

55 Sato, K. *et al.* Dynamic regulation of caveolin-1 trafficking in the germ line and embryo of Caenorhabditis elegans. *Mol Biol Cell* **17**, 3085-3094, doi:10.1091/mbc.e06-03-0211 (2006).

56 Mihaylova, V. T., Borland, C. Z., Manjarrez, L., Stern, M. J. & Sun, H. The PTEN tumor suppressor homolog in Caenorhabditis elegans regulates longevity and dauer formation in an insulin receptor-like signaling pathway. *Proc Natl Acad Sci U S A* **96**, 7427-7432, doi:10.1073/pnas.96.13.7427 (1999).

57 Cuentas-Condori, A. & Miller Rd, D. M. Synaptic remodeling, lessons from C. elegans. *J Neurogenet* **34**, 307-322, doi:10.1080/01677063.2020.1802725 (2020).

58 Wu, X. & Reddy, D. S. Integrins as receptor targets for neurological disorders. *Pharmacol Ther* **134**, 68-81, doi:10.1016/j.pharmthera.2011.12.008 (2012).
59 Moreno-Layseca, P. & Streuli, C. H. Signalling pathways linking integrins with cell cycle progression. *Matrix Biol* **34**, 144-153, doi:10.1016/j.matbio.2013.10.011 (2014).
60 Kowalski, J. R. *et al.* The Anaphase-Promoting Complex (APC) ubiquitin ligase regulates GABA transmission at the C. elegans neuromuscular junction. *Mol Cell Neurosci* **58**, 62-75, doi:10.1016/j.mcn.2013.12.001 (2014).
61 Cupolillo, D. *et al.* Autistic-Like Traits and Cerebellar Dysfunction in Purkinje Cell PTEN Knock-Out Mice. *Neuropsychopharmacology* **41**, 1457-1466, doi:10.1038/npp.2015.339 (2016).
62 Huang, W. C., Chen, Y. & Page, D. T. Genetic Suppression of mTOR Rescues Synaptic and Social Behavioral Abnormalities in a Mouse Model of Pten Haploinsufficiency. *Autism Res* **12**, 1463-1471, doi:10.1002/aur.2186 (2019).
63 Arden, K. C. FOXO animal models reveal a variety of diverse roles for FOXO transcription factors. *Oncogene* **27**, 2345-2350, doi:10.1038/onc.2008.27 (2008).
64 Santo, E. E. & Paik, J. FOXO in Neural Cells and Diseases of the Nervous System. *Curr Top Dev Biol* **127**, 105-118, doi:10.1016/bs.ctdb.2017.10.002 (2018).
65 McLaughlin, C. N. & Broihier, H. T. Keeping Neurons Young and Foxy: FoxOs Promote Neuronal Plasticity. *Trends Genet* **34**, 65-78, doi:10.1016/j.tig.2017.10.002 (2018).
66 de la Torre-Ubieta, L. *et al.* A FOXO-Pak1 transcriptional pathway controls neuronal polarity. *Genes Dev* **24**, 799-813, doi:10.1101/gad.1880510 (2010).
67 Khundrakpam, B. S., Lewis, J. D., Kostopoulos, P., Carbonell, F. & Evans, A. C. Cortical Thickness Abnormalities in Autism Spectrum Disorders Through Late Childhood, Adolescence, and Adulthood: A Large-Scale MRI Study. *Cereb Cortex* **27**, 1721-1731, doi:10.1093/cercor/bhx038 (2017).
68 Paik, J. H. *et al.* FoxOs cooperatively regulate diverse pathways governing neural stem cell homeostasis. *Cell Stem Cell* **5**, 540-553, doi:10.1016/j.stem.2009.09.013 (2009).
69 Byrne, A. B. *et al.* Insulin/IGF1 signaling inhibits age-dependent axon regeneration. *Neuron* **81**, 561-573, doi:10.1016/j.neuron.2013.11.019 (2014).
70 Cantello, R. *et al.* Ketogenic diet: electrophysiological effects on the normal human cortex. *Epilepsia* **48**, 1756-1763, doi:10.1111/j.1528-1167.2007.01156.x (2007).
71 Calderon, N., Betancourt, L., Hernandez, L. & Rada, P. A ketogenic diet modifies glutamate, gamma-aminobutyric acid and agmatine levels in the hippocampus of rats: A microdialysis study. *Neurosci Lett* **642**, 158-162, doi:10.1016/j.neulet.2017.02.014 (2017).
72 Yudkoff, M., Daikhin, Y., Horyn, O., Nissim, I. & Nissim, I. Ketosis and brain handling of glutamate, glutamine, and GABA. *Epilepsia* **49 Suppl 8**, 73-75, doi:10.1111/j.1528-1167.2008.01841.x (2008).
73 Newman, J. C. & Verdin, E. beta-Hydroxybutyrate: A Signaling Metabolite. *Annu Rev Nutr* **37**, 51-76, doi:10.1146/annurev-nutr-071816-064916 (2017).
74 Shimazu, T. *et al.* Suppression of oxidative stress by beta-hydroxybutyrate, an endogenous histone deacetylase inhibitor. *Science* **339**, 211-214, doi:10.1126/science.1227166 (2013).
75 Park, J., Lee, K., Kim, K. & Yi, S. J. The role of histone modifications: from neurodevelopment to neurodiseases. *Signal Transduct Target Ther* **7**, 217, doi:10.1038/s41392-022-01078-9 (2022).
76 Yamada, T., Zhang, S. J., Westerblad, H. & Katz, A. beta-Hydroxybutyrate inhibits insulin-mediated glucose transport in mouse oxidative muscle. *Am J Physiol Endocrinol Metab* **299**, E364-373, doi:10.1152/ajpendo.00142.2010 (2010).
77 Kim, D. H. *et al.* Anti-inflammatory action of beta-hydroxybutyrate via modulation of PGC-1alpha and FoxO1, mimicking calorie restriction. *Aging* **11**, 1283-1304, doi:10.18632/aging.101838 (2019).

78 McDaniel, S. S., Rensing, N. R., Thio, L. L., Yamada, K. A. & Wong, M. The ketogenic diet inhibits the mammalian target of rapamycin (mTOR) pathway. *Epilepsia* **52**, e7-11, doi:10.1111/j.1528-1167.2011.02981.x (2011).

79 Hertweck, M., Gobel, C. & Baumeister, R. C. elegans SGK-1 is the critical component in the Akt/PKB kinase complex to control stress response and life span. *Dev Cell* **6**, 577-588, doi:10.1016/s1534-5807(04)00095-4 (2004).

80 Meredith, R. M. Sensitive and critical periods during neurotypical and aberrant neurodevelopment: a framework for neurodevelopmental disorders. *Neurosci Biobehav Rev* **50**, 180-188, doi:10.1016/j.neubiorev.2014.12.001 (2015).

81 Kepler, L. D., McDiarmid, T. A. & Rankin, C. H. Rapid assessment of the temporal function and phenotypic reversibility of neurodevelopmental disorder risk genes in Caenorhabditis elegans. *Disease models & mechanisms* **15**, doi:10.1242/dmm.049359 (2022).

82 He, Y. *et al.* beta-Hydroxybutyrate as an epigenetic modifier: Underlying mechanisms and implications. *Heliyon* **9**, e21098, doi:10.1016/j.heliyon.2023.e21098 (2023).

83 Klockener, T. *et al.* High-fat feeding promotes obesity via insulin receptor/PI3K-dependent inhibition of SF-1 VMH neurons. *Nat Neurosci* **14**, 911-918, doi:10.1038/nn.2847 (2011).

84 Britton, J. S., Lockwood, W. K., Li, L., Cohen, S. M. & Edgar, B. A. Drosophila's insulin/PI3-kinase pathway coordinates cellular metabolism with nutritional conditions. *Dev Cell* **2**, 239-249, doi:10.1016/s1534-5807(02)00117-x (2002).

85 Kaplan, R. E. W., Webster, A. K., Chitrakar, R., Dent, J. A. & Baugh, L. R. Food perception without ingestion leads to metabolic changes and irreversible developmental arrest in C. elegans. *BMC Biol* **16**, 112, doi:10.1186/s12915-018-0579-3 (2018).

86 Baugh, L. R. To grow or not to grow: nutritional control of development during Caenorhabditis elegans L1 arrest. *Genetics* **194**, 539-555, doi:10.1534/genetics.113.150847 (2013).

87 Gems, D. *et al.* Two pleiotropic classes of daf-2 mutation affect larval arrest, adult behavior, reproduction and longevity in Caenorhabditis elegans. *Genetics* **150**, 129-155 (1998).

88 Baker, J., Liu, J. P., Robertson, E. J. & Efstratiadis, A. Role of insulin-like growth factors in embryonic and postnatal growth. *Cell* **75**, 73-82 (1993).

89 Brogiolo, W. *et al.* An evolutionarily conserved function of the Drosophila insulin receptor and insulin-like peptides in growth control. *Current biology : CB* **11**, 213-221, doi:10.1016/s0960-9822(01)00068-9 (2001).

90 Matuszek, B. *et al.* Increased serum insulin-like growth factor-1 levels in women with gestational diabetes. *Adv Med Sci* **56**, 200-206, doi:10.2478/v10039-011-0046-7 (2011).

91 Li, M. *et al.* The Association of Maternal Obesity and Diabetes With Autism and Other Developmental Disabilities. *Pediatrics* **137**, e20152206, doi:10.1542/peds.2015-2206 (2016).

Acknowledgments

Some strains were provided by the CGC, which is funded by NIH Office of Research Infrastructure Programs (P40 OD010440). We thank Mark Alkema, Michael Francis and Alex Byrne for strains. We thank Andrés Garelli, Guillermo Spitzmaul, Gabriela Salvador, Mark Alkema, Inés Carrera, Claire Bénard, Alexandra Byrne and Michael Francis for helpful discussions. In addition, we would like to acknowledge Ignacio Bergé, Adrian Bizet, Carolina Gomila, Marta Stulhdreher, María José Tiecher, Edgardo Buzzi and Carla Chrestía for technical support

Funding

This work was supported by Grants from: 1) Consejo Nacional de Investigaciones Científicas y Técnicas, Argentina to INIBIBB (PUE- N22920170100017CO) and to DR/ MJDR (PIP No. 11220200101606CO). 2) Agencia Nacional de Promoción de la Ciencia y la Tecnología ANPCYT Argentina to DR (PICT 2019-0480 and PICT-2021-I-A-00052) and MJDR (PICT-2017-0566 and PICT-2020-1734) and 3) Universidad Nacional Del Sur to DR (PGI: 24/B291) and MJDR (PGI: 24/B261). The funders had no role in the study design, data collection, and analysis, decision to publish, or preparation of the manuscript.

Conflict of Interest

The authors declare that the research was conducted in the absence of any commercial or financial relationships that could be construed as a potential conflict of interest.

Main Figures

Figure 1

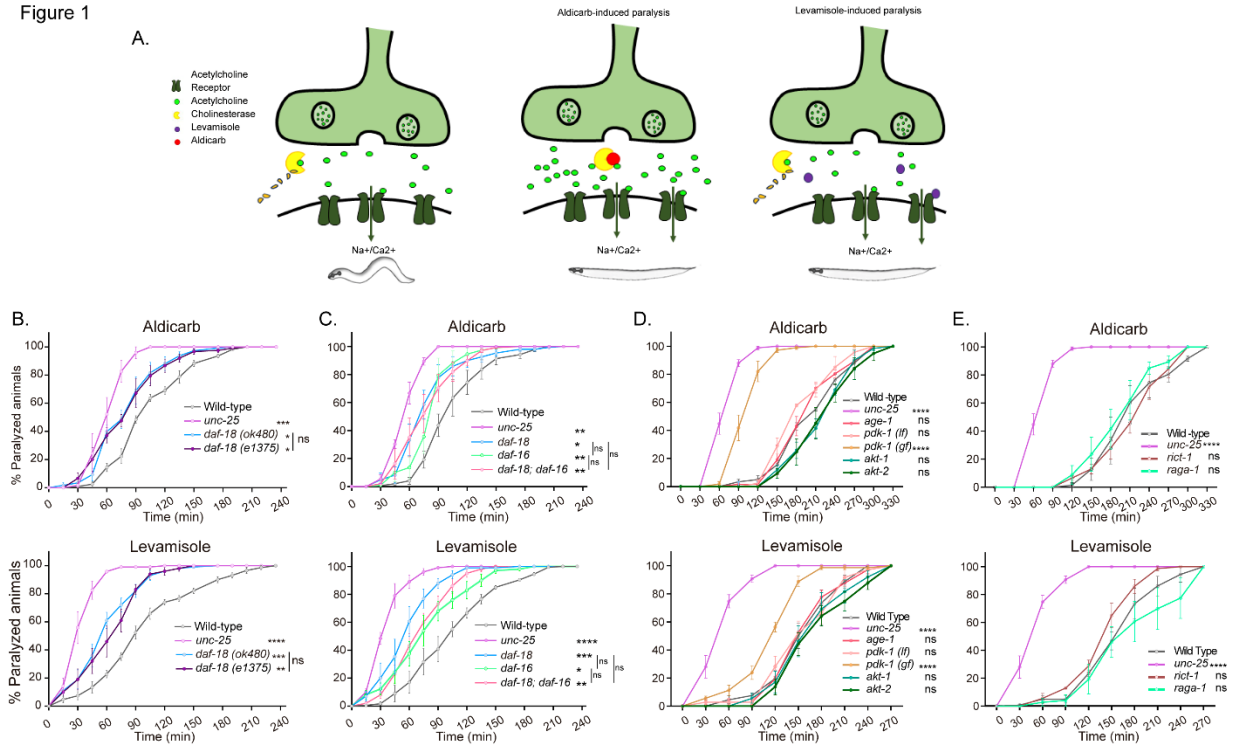

Figure 1. *daf-18/PTEN* mutants are hypersensitive to cholinergic drugs.

A. Schematic representation of paralysis induced by aldicarb and levamisole. Aldicarb acts by inhibiting acetylcholinesterase, leading to an accumulation of acetylcholine at the neuromuscular junction, resulting in continuous stimulation of muscles and worm paralysis. Levamisole functions as an agonist at nicotinic acetylcholine receptors, causing prolonged depolarization and, also, muscle paralysis. **B-E.** Quantification of paralysis induced by aldicarb (Top) and levamisole (Bottom). The assays were performed in NGM plates containing 2 mM aldicarb or 0.5 mM levamisole. Strains tested: N2 (wild-type) (B-E), CB1375 *daf-18(e1375)* (B), OAR144 *daf-18(ok480) (B-C)*, GR1310 *akt-1(mg144)* (D), TJ1052 *age-1(hx546)* (D), VC204 *akt-2(ok393)* (D), VC222 *raga-1(ok386)* (E) and KQ1366 *rict-1(ft7*) (E). All of these strains carry loss-of-function mutations. Furthermore, the strains denoted as "*pdk-1 (lf)*" and *"(gf)*" correspond

672 to JT9609 *pdk-1(sa680)*, which possesses a loss-of-function mutation, and GR1318 *pdk-*
673 *1(mg142)*, which harbors a gain-of-function mutation in the *pdk-1* gene, respectively. The strain
674 CB156 *unc-25(e156)* was included as a strong GABA-deficient control (B-D). At least four
675 independent trials for each condition were performed (n= 25-30 animals per trial). One-way ANOVA was used to test
676 statistical differences in the area under the curve (AUC) among different strains. Post-hoc analysis after One-
677 Way ANOVA was performed using Tukey's multiple comparisons test (B and C) and Dunnet´s to
678 compare against the wild-type strain (D and E) (ns $p > 0.05$; * $p \leq 0.05$; ** $p \leq 0.01$; *** $p \leq$
679 0.001; **** $p \leq 0.0001$).
680

681 **Figure 2**

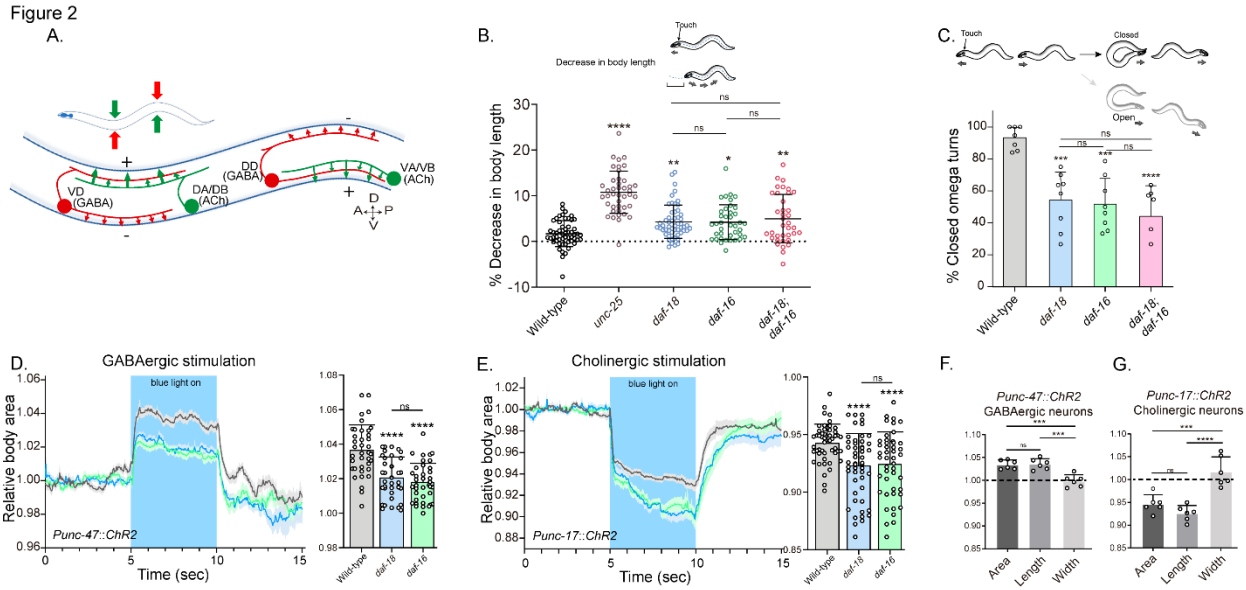

682

683

684 **Figure 2. *daf-18/PTEN* mutants exhibit phenotypes typical of GABA-deficient animals.**

685 **A.** Schematic of *C. elegans* adult neuromuscular circuit. Red indicates GABAergic motor
686 neurons (DD/VD) and green indicates cholinergic motor neurons (VA/VB and DA/DB). The VA
687 and VB cholinergic motor neurons send synaptic inputs to the ventral body wall muscles and the
688 DD GABAergic motor neurons. The release of ACh from VA/VB neurons leads to the contraction
689 of the ventral body wall muscles and the activation of DD GABAergic motor neurons that
690 release GABA on the opposite side of the worm, causing relaxation of the dorsal body wall
691 muscles. Conversely, activation of the DA and DB cholinergic motor neurons produces
692 contraction of the dorsal body wall muscles and activates the VD GABAergic motor neurons.
693 The VD GABAergic motor neurons release GABA, causing relaxation of the ventral body wall
694 muscles, and thus contralateral inhibition. **B.** Quantification of body shortening in response to
695 anterior touch. Data are represented as mean ± SD. n= 50-70 animals per genotype distributed
696 across four independent experiments. Kruskal-Wallis analysis with Dunn's post-test for multiple

comparisons was performed. **C.** (Top) Scheme of *C. elegans* escape response in NGM agar. After eliciting the escape response by an anterior gentle touch, the omega turns were classified as closed (head and tail are in contact) or open (no contact between head and tail). (Bottom) Quantification of % closed omega turns/ total omega turns. At least six independent trials for each condition were performed (n= 20-25 animals per genotype/trial). Data are represented as mean ± SD. One-way ANOVA with Tukey's post-test for multiple comparisons was performed. **D-E.** Light-evoked elongation/contraction of animals expressing Channelrhodopsin (ChR2) in GABAergic (D) and Cholinergic (E) motorneurons. Animals were filmed before, during, and after a 5-second pulse of 470 nm light stimulus (15 frames/s). The body area in each frame was automatically tracked using a custom FIJI-Image J macro. The averaged area of each animal during the first 125 frames (0-5 s) established a baseline for normalizing light-induced body area changes. To compare the changes induced by optogenetic activity between different strains, the body area measurements for each animal were averaged from second 6 (1 second after the blue light was turned on) to second 9 (1 second before the light was turned off). These mean ± SD values are depicted in the bar graph shown to the right of each trace representation (n=40-55 animals per genotype). Tukey´s multiple comparisons method following One-Way ANOVA was performed for D, while Dunn's multiple comparisons test after Kruskal-Wallis analysis was used in E. **F-G.** Manual Measurement of Body length and width upon Optogenetic Stimulation of GABAergic (F) and Cholinergic (G) neurons. At the 2.5-second time point of light stimulation, we manually measured both the width and length of multiple animals and compared these measurements with the corresponding areas obtained from automated analysis (see Materials and Methods). The width of the worms remained relatively constant, highlighting that the alterations in body area primarily stem from changes in the animal's length. One-way ANOVA with Tukey's post-test for multiple comparisons was performed. Data are shown as mean ± SD. (ns $p > 0.05$; * $p \leq 0.05$; ** $p \leq 0.01$; *** $p \leq 0.001$; **** $p \leq 0.0001$).

723 **Figure 3**

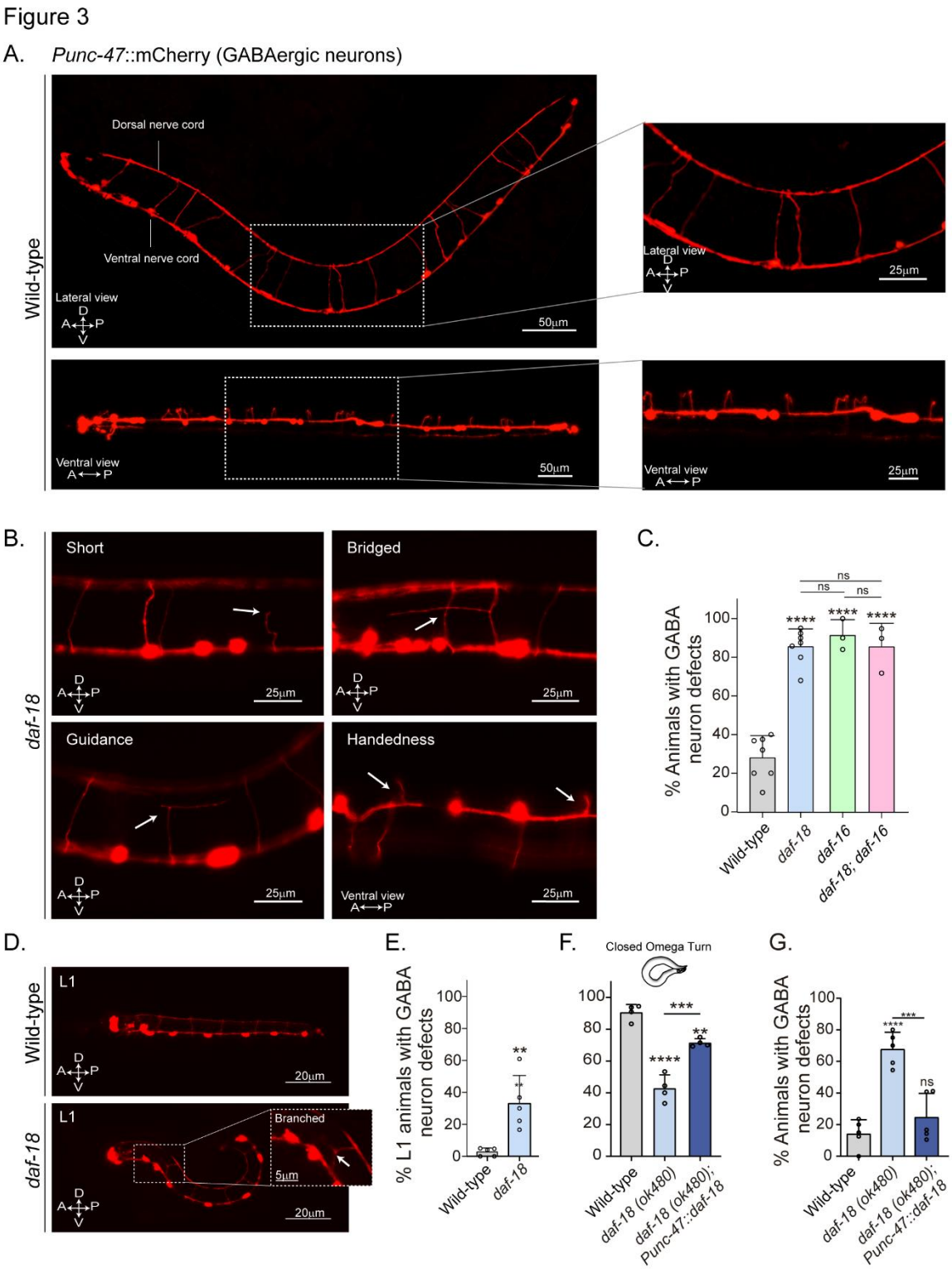

724

Figure 3. *daf-18/PTEN* mutants show neurodevelopmental defects in GABAergic motor -neurons.

A. Representative images of wild-type animals expressing *mCherry* in the GABAergic motor neurons are shown laterally (Top) and ventrally (Bottom). In the insets, commissures are depicted at a higher resolution. Note that in the ventral view, all the processes travel through the right side of the animal's body. **B.** Representative images of commissure defects observed in *daf-18 (ok480)* mutants (arrows). The defects shown are: Short, commissure length less than half of nematode width; Bridged, neighboring commissures linked by a neurite; Guidance, commissures that do not reach dorsal nerve cord; and Handedness, commissure running along the opposite side of the animal's body. **C.** Quantification of GABAergic system defects. Each bar represents the mean ± SD. One-way ANOVA and Tukey's multiple comparisons test were used for statistics (ns $p > 0.05$; **** $p \leq 0.0001$). At least three independent trials for each condition were performed (n: 20-25 animals per genotype/trial). **D.** Representative image of L1 animals (1 h post-thatch) expressing *Punc-47::mCherry* in wild-type (Top) and *daf-18(ok480)* mutant (Bottom) backgrounds. In this larval stage, only six GABAergic DD motor neurons are born. The inset shows a typical defective (branched) commissure. **E.** Quantification of GABAergic system defects in L1s. Each bar represents the mean ± SD. Two-tailed unpaired Student's t test. (**$p \leq 0.01$). At least five independent trials for each condition were performed (n: ~20 animals per genotype/trial). **F-G.** Quantification of closed omega turns/total omega turns and commissure defects in GABAergic neurons of animals expressing *daf-18/PTEN* solely in GABAergic neurons. One-way ANOVA and Tukey's multiple comparisons test were used for statistics (ns $p > 0.05$; **$p \leq 0.01$; *** $p \leq 0.001$; **** $p \leq 0.0001$). At least four independent trials for each condition were performed (n: 15-20 animals per genotype/trial)

A-Anterior; P-Posterior; D-Dorsal; V-Ventral.

750 **Figure 4**

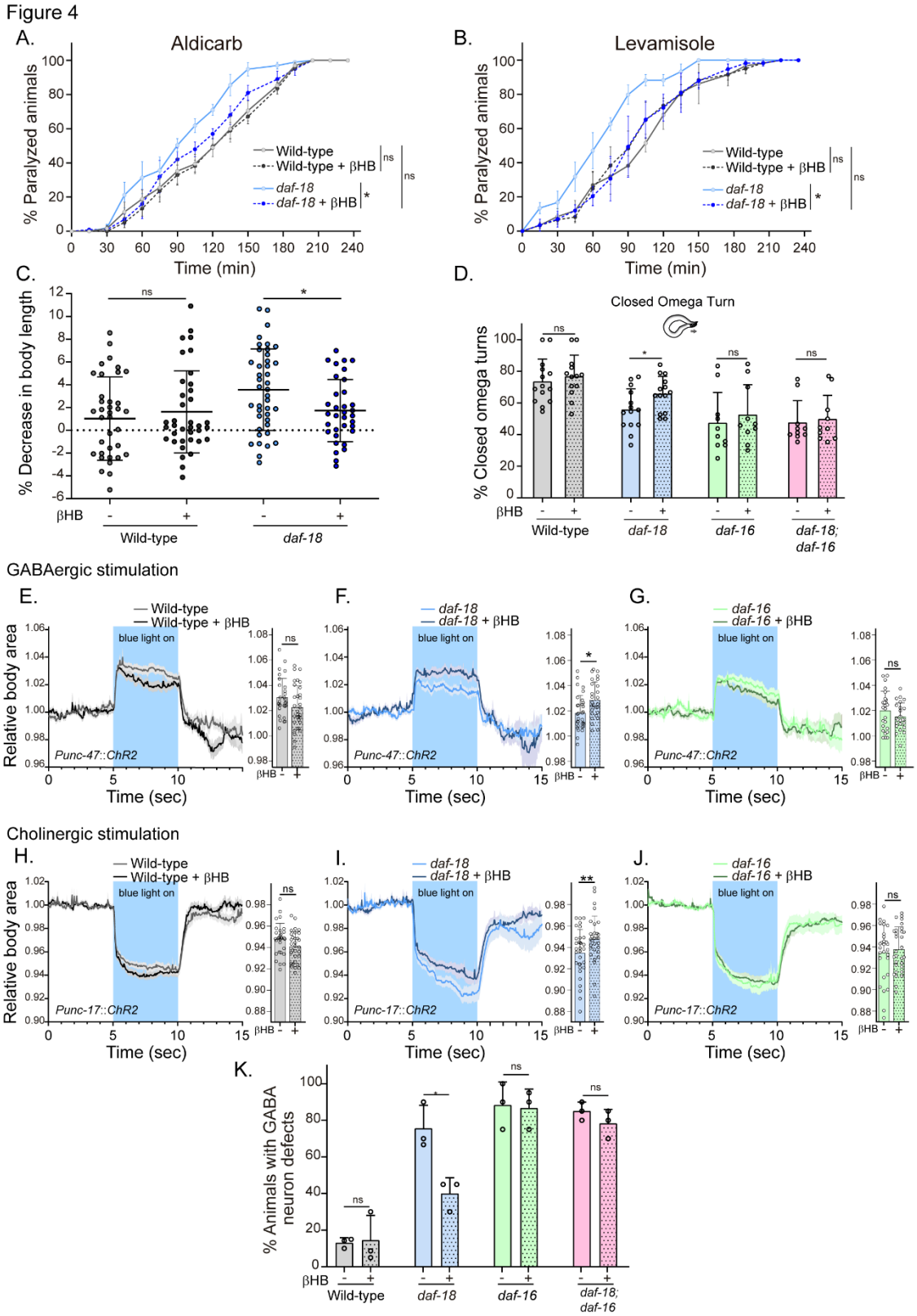

751

Figure 4. Dietary βHB supplementation ameliorates GABAergic deficits in *daf-18/PTEN* mutants.

Animals were exposed to βHB (20 mM) throughout development (from embryo to L4/young adults). **A and B.** Quantification of paralysis induced by cholinergic drugs. At least four independent trials for each condition were performed (n: 20-25 animals per genotype/trial). Two-tailed unpaired Student's t-test (ns $p > 0.05$; *$p \leq 0.05$; ** $p \leq 0.01$) was used to compare βHB treated and untreated animals. **C.** Measurement of body length in response to anterior touch. n= 30-40 animals per genotype distributed across three independent experiments. Two-tailed unpaired Student's t-test was used to compare βHB treated and untreated animals (ns $p > 0.05$; * $p \leq 0.05$). **D**. Quantification of closed omega turns/total omega turns during the escape response. At least eight independent trials for each condition were performed (n= 20 animals per genotype/trial). Results are presented as mean ± SD. Two-tailed unpaired Student's t test (ns $p > 0.05$; *$p \leq 0.05$). **E-J.** Light-evoked elongation/contraction of animals expressing ChR2 in GABAergic (E-G) and cholinergic (H-J) motorneurons. The mean body area (mean ± SD) during 3 seconds of the light pulse is depicted in the bar graph shown to the right of each trace representation (see figure 2) (n=25-35 animals per condition). Two-tailed unpaired Student's t-test (ns $p > 0.05$; *$p \leq 0.05$; ** $p \leq 0.01$). **K.** Quantification of commissure defects in GABAergic neurons. Results are presented as mean ± SD. Two-tailed unpaired Student's t-test (ns $p > 0.05$; *$p \leq 0.05$). At least three independent trials for each condition were performed (n= ~20 animals per genotype/trial).

Figure 5

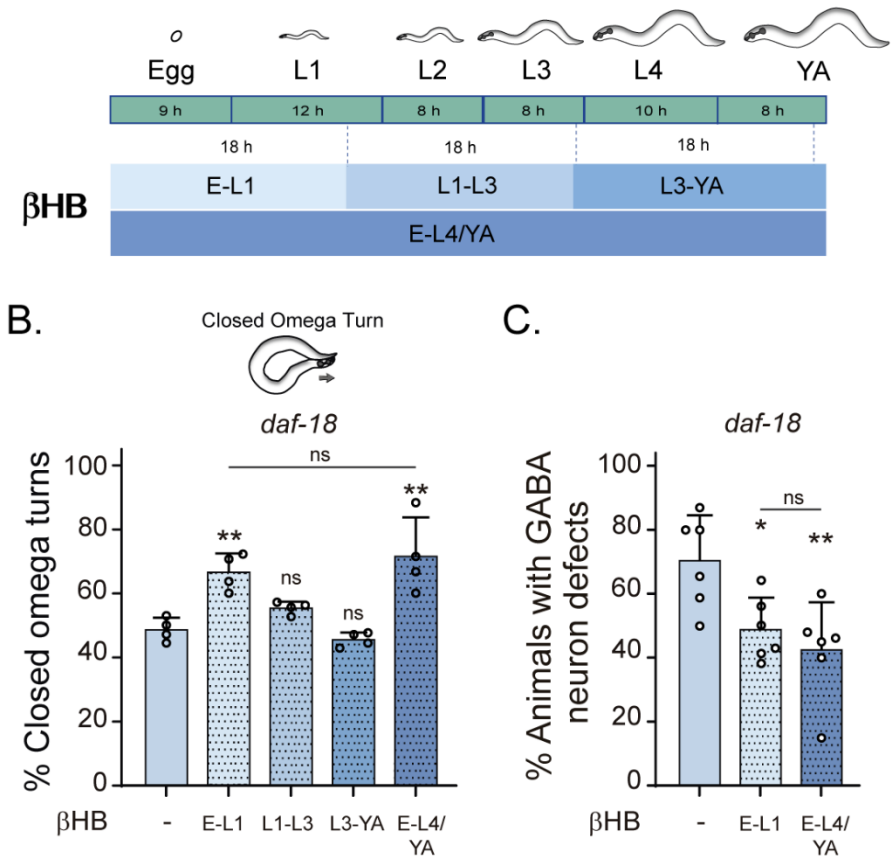

Figure 5. Early developmental stages are critical for βHB-modulation of GABAergic signaling.

A. Animals were exposed to βHB-enriched diet for 18-h periods at different developmental stages: i) E-L1 covered *ex-utero* embryonic development (~ 9 h) and the first 8-9 h of the L1 stage; ii) L1-L3 covered the latter part of the L1 stage (~3-4 h), the entire L2 stage (~8 h), and most of the L3 stage (~6-7 h), iii) L3-YA(Young Adult) spanned the latter part of the L3 stage (~ 1-2 h), the entire L4 stage (~10 h), and the first 6-7 h as adults, and iv) E-L4/YA implies exposure throughout development (from embryo to Young Adult). **B-C.** Quantification of closed omega turns/total omega turns in *daf-18/PTEN* (B) and GABAergic commissure defects (C) in *daf-18/PTEN* mutants exposed to βHB at different developmental intervals. Four and six independent trials for each

784 condition were performed in B and C, respectively (n=: 20-25 animals per genotype/trial).

785 Results are presented as mean ± SD. One-way ANOVA with Tukey's post-test for multiple

786 comparisons was performed (ns $p > 0.05$; *$p \leq 0.05$; ** $p \leq 0.01$).

787

788 **Graphical Abstract**

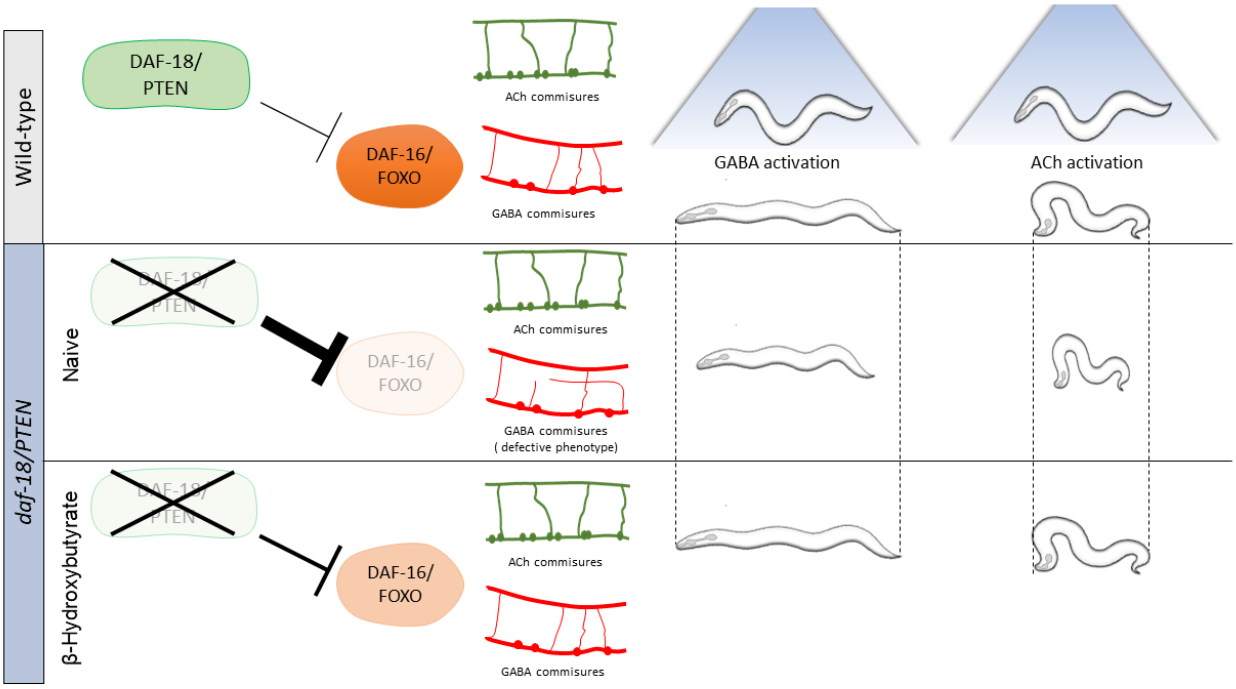

789

790

Materials and methods

***C. elegans* culture and maintenance.** All *C. elegans* strains were grown at room temperature (22ºC) on nematode growth media (NGM) agar plates with OP50 *Escherichia coli* as a food source. The wild-type reference strain used in this study is N2 Bristol. Some of the strains were obtained through the *Caenorhabditis* Genetics Center (CGC, University of Minnesota). Worm population density was maintained low throughout their development and during the assays. All experiments were conducted on age-synchronized animals. This was achieved by placing gravid worms on NGM plates and removing them after two hours. The assays were performed on the animals hatched from the eggs laid in these two hours.

Transgenic strains were generated by microinjection of plasmid DNA containing the construct *Punc-47::daf-18cDNA* (kindly provided by Alexandra Byrne, UMASS Chan Medical School) at 20 ng/µL into the germ line of (*daf-18 (ok480); lin-15 (n765ts*)) double mutants with the co-injection marker *lin-15* rescuing plasmid pL15EK (80 ng/µl). At least three independent transgenic lines were obtained. Data are shown from a single representative line.

The strains used in this manuscript were:

CB156 *unc-25(e156*) III

MT6201 *unc-47(n2409*) III

CB1375 *daf-18(e1375*) IV

OAR144 *daf-18(ok480*) IV

GR1307 *daf-16(mgdf50)* I

OAR115 *daf-16(mgDf50)* I*; daf-18(ok480)* IV

OAR161 *daf-18(ok480)*; *wpEx173[Punc-47::daf-18 + myo-2::GFP]*

LX929 *vsIs48[Punc-17::gfp]*

IZ629 *ufIs34[Punc-47::mCherry]*

OAR117 *ufIs34[Punc-47::mCherry; daf-18(ok480]*

OAR118 *vsIs48[Punc-17::GFP); daf-18(ok480)]*

817 OAR142 *ufis34[Punc-47::mCherry; daf-16(mgDf50)]*

818 OAR143 *ufis34 [Punc-47::mCherry; daf-16(mgDf50); daf-18(ok480)]*

819 CF1553 *muIs84[(pAD76) Psod-3::gfp + rol-6(su1006)]*

820 OAR140 *muIs84[(pAD76) Psod-3::gfp + rol-6]; daf-18(ok480)*

821 OAR141 *muIs84[(pAD76) Psod-3::gfp + rol-6]; daf-16(mgDf50)*

822 OH99 *mgIs18[Pttx-3::gfp]*

823 OAR83 *daf-18(ok480); mgIs18[Pttx-3::gfp]*

824 MT13471 *nIs121[Ptph-1::gfp]*

825 OAR112 *nIs121[Ptph-1::gfp]; daf-18(ok480)*

826 IZ805 *ufIs53[Punc-17::ChR2]*

827 ZM3266 *zxIs3[Punc-47::ChR2::YFP]*

828 OAR177 *ufIs53[P*unc-17::ChR2;;YFP*]; daf-18(ok480)*

829 OAR178 *ufIs53[P*unc-17::ChR2::YFP*] ; daf-16(mgDf50)*

830 OAR179 *zxIs3[Punc-47::ChR2::YFP];daf-18(ok480)*

831 OAR180 *zxIs3[Punc-47::ChR2::YFP] ; daf-16(mgDf50)*

832 TJ1052 *age-1(hx546)*

833 GR1310 *akt-1(mg144)*

834 GR1318 *pdk-1(mg142)*

835 JT9609 *pdk-1(sa680)*

836 VC204 *akt-2(ok393)*

837 *VC222 raga-1(ok386)*

838 KQ1366 *rict-1(ft7)*

839

840 **Paralysis assays.** Paralysis assays were carried out in standard NGM plates with 2 mM

841 aldicarb (Sigma-Aldrich) or 0.5 mM levamisole (Alfa Aesar). 25-30 L4 worms were transferred to

each plate and paralyzed animals were counted every 15 or 30 minutes. An animal was considered paralyzed when it did not respond after prodding three times with a platinum wire on the head and tail[1]. At least four independent trials with 25-30 animals for each condition were performed. The area under the curve (AUC) for each condition in each experiment was used for statistical comparisons

Escape response. Escape response assays were performed on NGM agar plates seeded with a thin bacterial lawn of OP50 *E. coli.* To maintain tight control of growth and moisture, 120 μL of bacteria were seeded 24 hours before the assay and grown overnight at 37º C. The day of the assay, young adult worms were transferred to the plates and allowed to acclimate for at least 5 min. Omega turns were induced by gentle anterior touch with fine eyebrow hair and were classified as closed when the worm touched the tail with its head as previously described [2]. Between 4 and 7 independent trials with ~20 animals for each condition were performed.

Body length assays. Body length measurements were performed in standard NGM agar plates without bacteria. Young adult synchronized worms were transferred into the plates and allowed to acclimate for at least 5 min. Worms were recorded with an Amscope Mu300 camera. Animal body length, before and after touching with a platinum pick, was measured using FIJI Image J software. Quantification of body shortening after touching was calculated as the decrease of body length related to the length of the animal before being touched.

Commissure analysis. Synchronized L1 or L4 animals carrying the fluorescence reporters *vsIs48* (*Punc-17::GFP*, cholinergic neurons) or *uflS34* (*Punc-47::mCherry*, GABAergic neurons) were immobilized with sodium azide (0.25 M) on 2% agarose pads. Commissures of GABAergic and cholinergic neurons were scored with a Nikon Eclipse TE 2000 fluorescence microscope. A commissure is generally composed of a single process, and occasionally two neurites that extend together dorsally. Defects on commissures, including guidance defects, abnormal branching, and incomplete commissures were classified similarly to previous reports [3]. The

867 percentage of animals with at least one commissure defect was calculated for each neuronal
868 class (e.g., cholinergic or GABAergic). At least three trials (~20 animals per condition in each
869 trial) were analyzed for each individual experiment. Representative images shown in the figures
870 were collected using laser confocal microscopy (ZEISS LSM 900 with AirScan II) with 20× and
871 63× objectives.

872 **β-hydroxybutyrate assays.** Worms were exposed to 20 mM DL-3-hydroxybutyric acid sodium
873 salt (Acros Organics) on NGM agar plates seeded with *E. coli* OP50. We synchronized the
874 animals similarly to other experiments by placing gravid animals in NGM plates containing 20
875 mM of βHB and removing them after two hours.

876 For experiments involving exposure at different developmental stages, animals were transferred
877 between plates with and without βHB as needed. For the earliest exposure, eggs were laid on
878 plates containing 20 mM of βHB and then transferred to drug-free plates to complete their
879 development. Conversely, for later exposures, animals were born on βHB-free plates and
880 subsequently transferred to βHB-containing plates at the specified time (See Figure 5).

881 ***sod-3* expression.** *sod-3* expression levels were analyzed in transgenic strains containing the
882 transcriptional reporter *muIs84*, as described previously [4,5]. Synchronized L4 animals were
883 anesthetized with Sodium Azide (0.25 M) and mounted on 2% agarose pads. Images were
884 collected using a Nikon Eclipse TE 2000 fluorescence microscope. GFP fluorescence intensity
885 was quantified in same-sized ROIs at the head of the animal using Image J FIJI software.
886 Results were normalized to control conditions (wild-type individuals without βHB). ~35-60
887 animals for each genotype/condition were analyzed.

888 **Optogenetic assays.** We examined young adult animals (6-8 hours post-L4 stage) that express
889 Channelrhodopsin (ChR2) in either GABAergic (*Punc-47::ChR2*) or cholinergic neurons (*Punc-*
890 *17::ChR2*). We transferred these animals to a NGM 6mm agar plate without food, let them

acclimate for 5 minutes, and recorded each animal at 15 frames per second using an Allied Vision Alvium 1800 U-500m camera. To stimulate neuronal activity, we exposed the animals to 470 nm light pulses for 5 seconds. These light pulses were delivered using a custom Python script (VIMBA Peron) to an Arduino Uno microcontroller, which operated a Mightex compact universal LED controller (Mightex SLC-MA02-U). The light emission was achieved through a Mightex High-Power LED Collimator Source (LCS-0470–03-11). To precisely track the changes in the worm's body, we continuously monitored its area from 5 seconds before the light stimulus, during the light stimulus and until 5 seconds afterward. We developed a FIJI-Image J macro capable of automatically tracking the body area in each frame, capitalizing on the clear contrast between the worm's body and the background. As demonstrated in Movies 3 and 4, changes in body area directly corresponded to alterations in the animal's length. To compare the changes induced by optogenetic activity between different strains, the body area measurements for each animal were averaged from second 6 (1 second after the blue light was turned on) to second 9 (1 second before the light was turned off). These average values were used for the statistical comparisons detailed in each figure legend.

To validate our measurement system, we manually measured the width of 6-8 animals at the 2.5-second point of light stimulation and compared them to the body area and length. Our observations consistently showed that, regardless of whether the area increased or decreased (depending on the activation of GABAergic or cholinergic neurons), the width remained mostly unchanged (Figure 2F and 2G). Therefore, the observed changes in the animal´s area measured by our FIJI-Image J macro indeed represent alterations in the animal's length.

AIY and HSN analysis. Synchronized L4 or Young Adult worms carrying the fluorescence reporters *Pttx-3::gfp* (AIY interneurons expressing GFP) and *Ptph-1::gfp* (HSN expressing GFP) were immobilized with sodium azide (0.25 M) on 2% agarose pads and analyzed with a Nikon Eclipse TE 2000 fluorescence microscope. AIY neurons morphology were sorted in qualitative

categories (see figure legend) while the migration of HSN was classified in quantitative categories using ImageJ software.

Statistical Analysis. The results presented in each figure are the average of at least three independent assays. Bars represent mean ± SD. Typically, one-way ANOVA was employed for analyzing multiple parametric samples, and Tukey's post hoc test was used for pairwise comparisons among all groups. For comparisons against a control group, Dunnett's post hoc test was used. For multiple non-parametric samples, the Kruskal-Wallis test was applied followed by Dunn's post hoc test, which was also utilized for comparisons against the control group. In cases where comparisons were made between two independent conditions, a t-test was utilized for parametric data, while the Mann-Whitney U test was employed for non-parametric data. We used the software GraphPad Prism version 6.01 to perform statistics. The statistical information is indicated in the figure legends. For all assays, the scoring was done blinded. All raw data are available in Open Science Framework (https://osf.io/mdpgc/?view_only=3edb6edf2298421e94982268d9802050).

Supplementary Figure 1

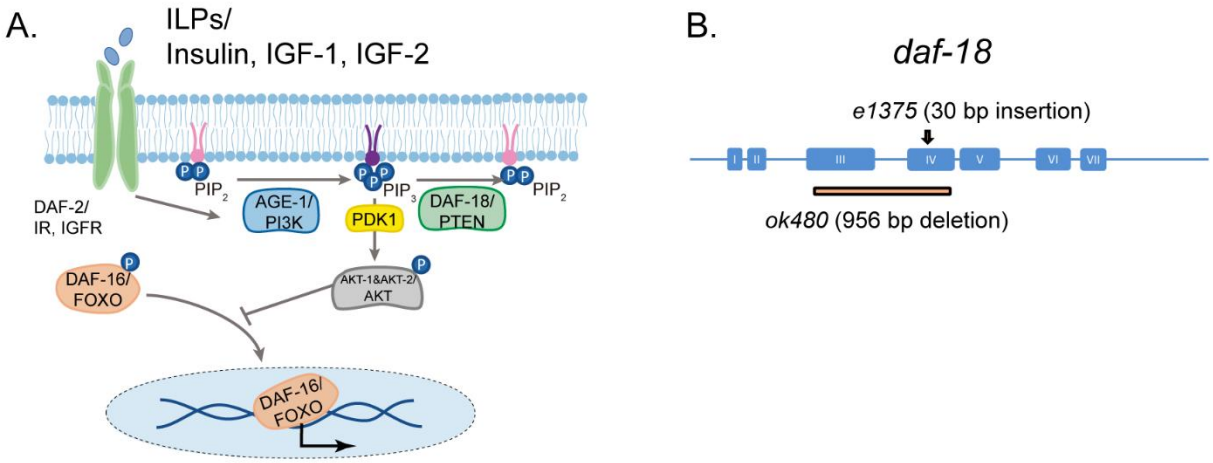

Supplementary Figure 1. ***daf-18/PTEN is the negative modulator of the PI3K/AKT pathway*****.** **A.** *daf-18/PTEN* encodes a lipid and protein phosphatase that hydrolyzes phosphatidylinositol (3,4,5)-trisphosphate (PIP_3) to phosphatidylinositol-4,5-bisphosphate (PIP_2). It is the main negative modulator of PDK and AKT activity. In *daf-18/PTEN* mutants, AKT is overactivated leading to high levels of DAF-16/FOXO phosphorylation that prevents the translocation of this transcription factor to the nucleus. **B.** Gene structure of *daf-18*. Coding sequences are represented by blue boxes. The *daf-18(e1375)* mutant allele inserts a 30 bp sequence in exon IV. This insertion occurs downstream of the phosphatase catalytic domain and causes a frameshift that leads to premature truncation of the protein. This *e1375* mutation partially reduces DAF-18 function. The *daf-18(ok480)* allele contains a 956 bp deletion that removes most of exon 3 and exon 4 and is generally considered to be a null allele.

Supplementary Figure 2

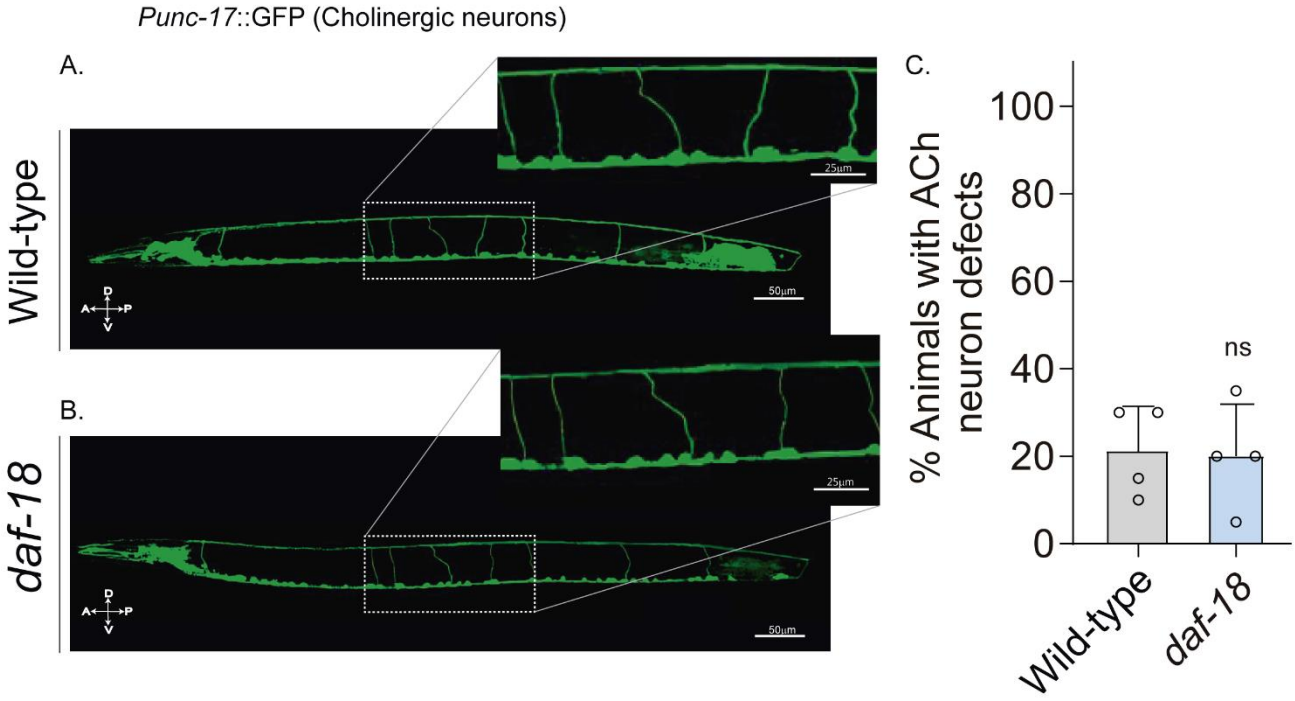

946

947 **Supplementary Figure 2. *daf-18/PTEN* mutations do not affect excitatory cholinergic**

948 **motor-neuron morphology**

949 **A.** Representative images of animals expressing GFP in the cholinergic neurons. In the insets,

950 the commissural processes can be appreciated with higher resolution. **B**. Quantification of

951 cholinergic system defects. Each bar represents the mean ± SD for at least four trials (~ 20

952 animals per trial). Statistical significance between the strains was determined by two-tailed

953 unpaired Student's t-test. (ns $p > 0.05$).

954 A anterior; P Posterior; D Dorsal; V Ventral.

955

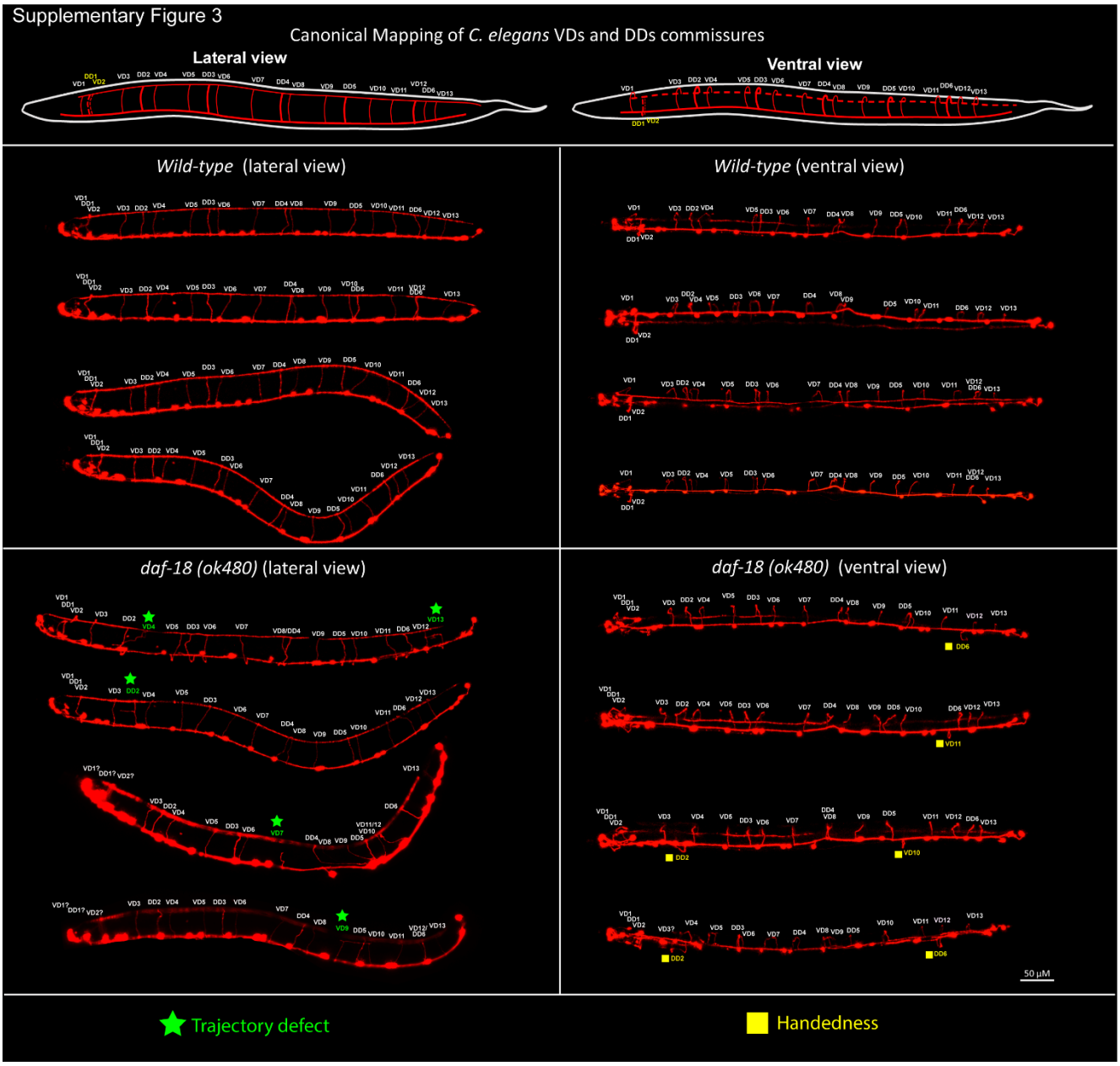

Supplementary Figure 3. *daf-18/PTEN* deficiencies affect DDs and VDs GABAergic neurons

Top, schematic representation of the location of the commissures belonging to the two types of GABAergic neurons in lateral and ventral views (based on[6,7]). **Below**, representative images of wild-type and *daf-18(ok 480)* worms viewed laterally (left) and ventrally (right). Note that in both lateral and ventral views (handedness errors) defects appear in both DDs and VDs neurons.

964 Errors in the first 3 commissures were not considered due to the difficulty of identifying the

965 commissures corresponding to VD1, DD1, and VD2 neurons.

966

Supplementary Figure 4

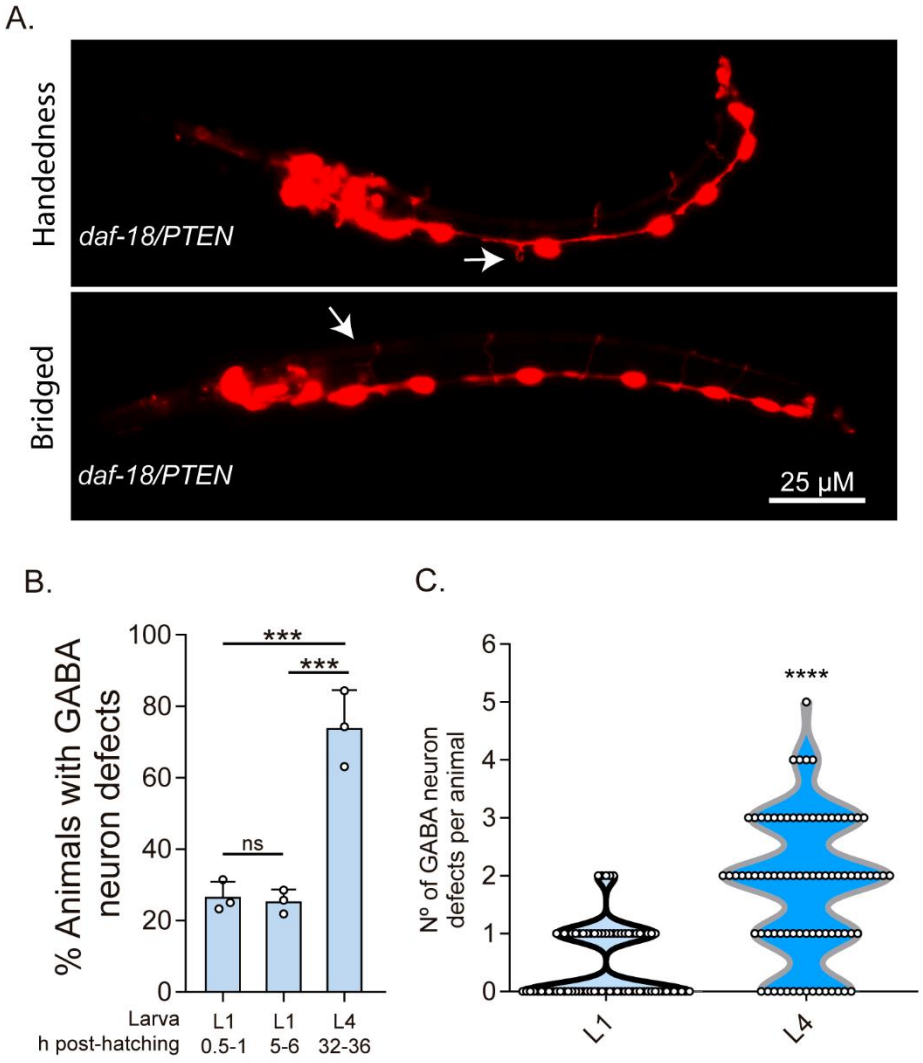

967

968 **Supplementary Figure 4.** ***DD-GABAergic neurons show defects in recently hatched L1***

969 ***animals of daf-18/PTEN mutants***

970

971 **A**. Representative images of the most common errors observed in L1 animals (1 h post-hatch)

972 of *daf-18* mutants. These types of defects, plus others such as short commissures and guidance

973 defects, are also observed in L4 animals (Figure 3 and S3). **B**. GABAergic commissure defects

974 were quantified in *daf-18/PTEN* mutants at various developmental stages: 0.5-1 h post-hatching

975 (early L1 larva), 5-6 h post-hatching (mid-L1 larva), and L4 stage (32-36 h post-hatching). Three

976 independent trials for each condition were performed, with at least 30 animals per condition/trial.
977 Results are presented as mean ± SD. A one-way ANOVA with Tukey's post-hoc test was used
978 (ns $p > 0.05$; **$p \leq 0.01$; *** $p \leq 0.001$; **** $p \leq 0.0001$). **C**. Quantification of the number of errors
979 per animal in L1 and L4 larvae. Statistical significance was determined by Mann Whitney test
980 (**** $p \leq 0.0001$; n=75-80)

981

Supplementary Figure 5

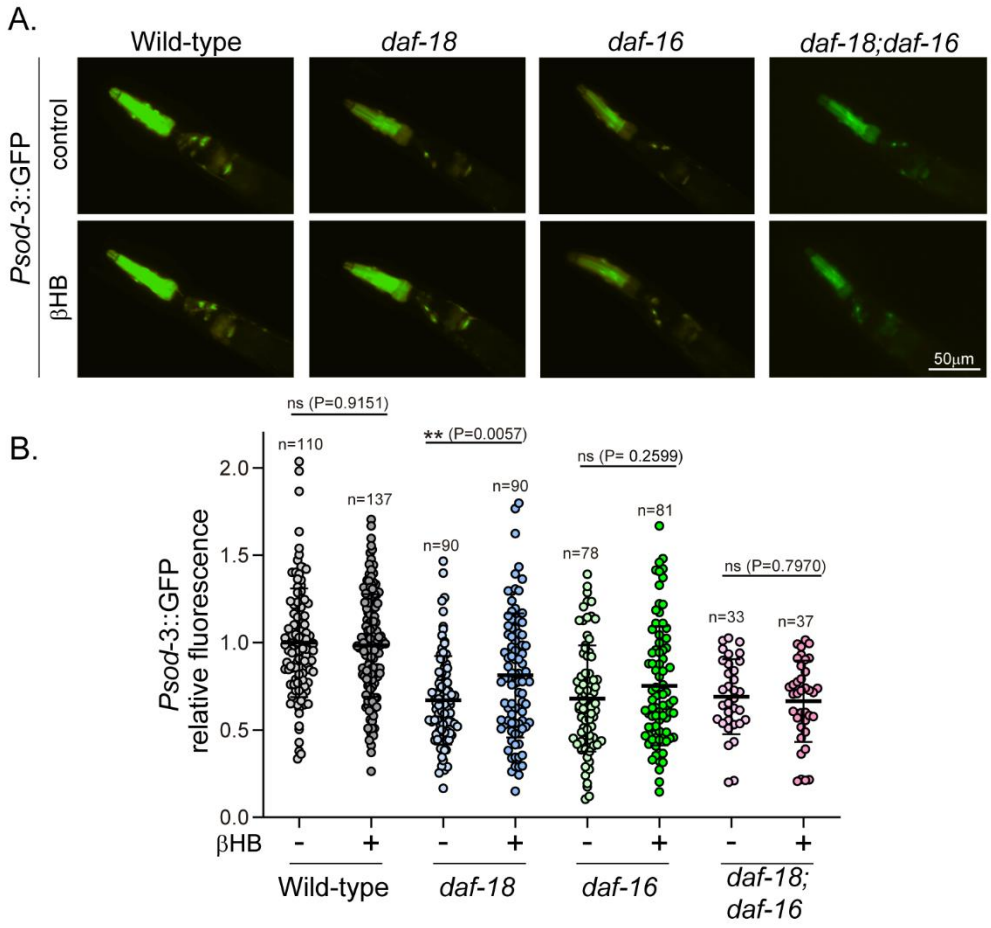

Supplementary Figure 5. Exposure to βHB induces *sod-3* expression in *daf-18/PTEN*, but not in *daf-16/FOXO* mutants.

A. Representative fluorescence images (20X magnification) of worms expressing *Psod-3::GFP* in different genetic backgrounds (wild-type, *daf-18(ok480)*, *daf-16(mgDf50) and daf-18(ok480); daf-16(mgDf50))* upon exposure to βHB (20mM). **B.** Corresponding quantification of the fluorescence intensity per animal in the head. Scatter dot plot (line at the median) with the relative expression of *Psod-3::GFP* normalized to naïve wild-type animals. Statistical significance between the treatment and the corresponding control was determined by Mann Whitney test (ns $p > 0.05$; ** $p \leq 0.01$; **** $p \leq 0.0001$, n= 40-90).

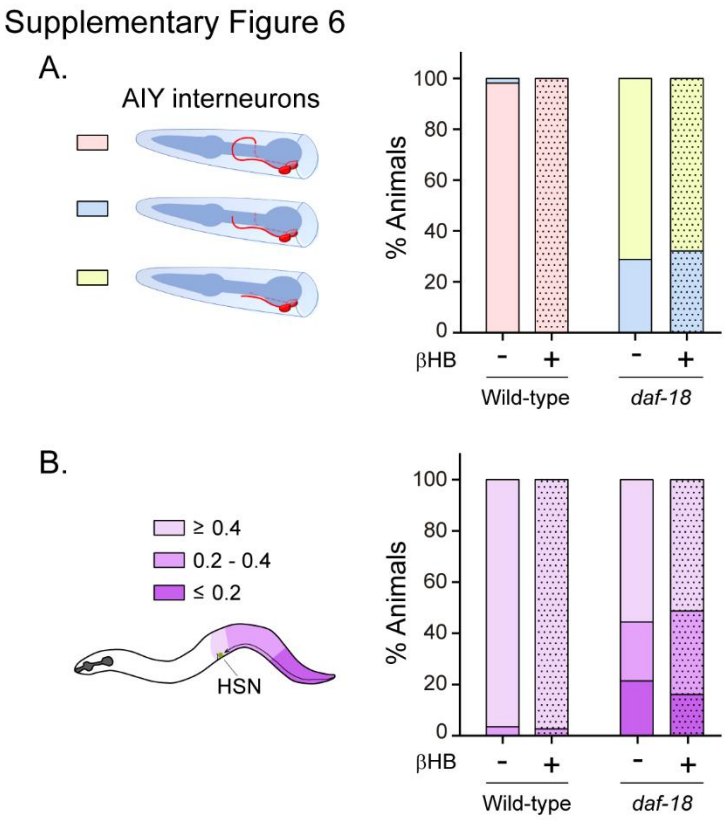

Supplementary Figure 6. βHB does not prevent neurodevelopmental defects in AIY and HSN neurons.

A. AIY processes were visualized in transgenic animals expressing cytoplasmic *GFP* in AIY neurons (*Pttx-3b::GFP*) in wild-type and *daf-18(ok480)* mutant backgrounds. AIY neuronal growth defects were quantified as described before (Christensen *et al*., 2011). Left: Scheme of AIY morphology and location in the nematode nerve ring. Blue, pharynx; red, AIY interneurons. Pink: wild-type AIY morphology. The two interneurons meet at the dorsal midline. Light blue and yellow: denote different levels of AIY neurite truncation. Right: Percentage of animals with truncated neurites in wild-type and *daf-18(ok480)* mutants under exposure (or not) to βHB (20 mM). **B.** HSN were visualized in transgenic animals expressing *GFP* in serotonergic neurons (*Ptph-1::GFP*) in wild-type and *daf-18(ok480)* mutant backgrounds. HSN under-migration defects were identified as described before (Kennedy et al., 2013). Left: Schematic representation of the HSN migratory route during embryogenesis and the corresponding

location of the HSN (green circle) in a young adult animal. Only one of two bilaterally symmetric HSNs is illustrated. Colors show information about the position of HSNs: Light purple: complete migration (≥ 0.4), middle purple: intermediated migration (>0.2-<0.4), dark purple: unmigrated (≤0.2). Right: Quantification of the percentage of animals with different HSN migration positions (the most under-migrated neuron of each animal is considered). Bars represent the mean values of at least three independent experiments. Note that there is no significant effect with βHB treatment compared to controls.

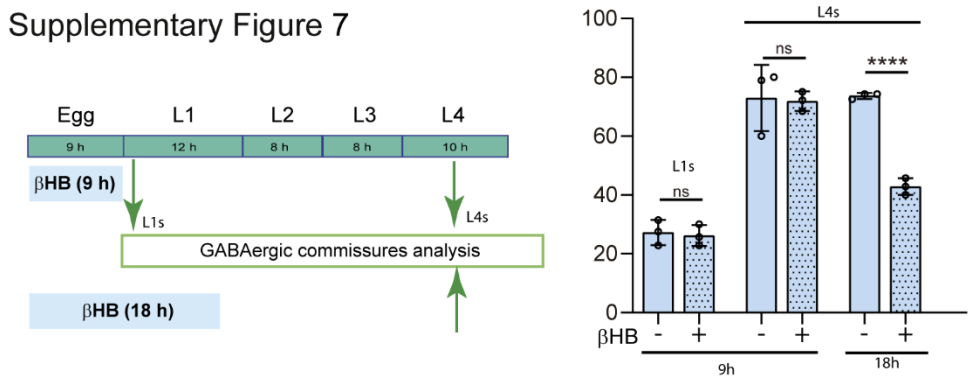

Supplementary Figure 7. βHB does not prevent neurodevelopmental defects in GABAergic neurons when applied exclusively during *ex-utero* embryonic development.

Quantification of GABAergic commissure defects in L4-stage of *daf-18/PTEN* mutant animals exposed to βHB during the first 9 h post-egg laying (just before hatching) and 18 hours post-egg laying. The animals were then transferred to control plates without βHB and maintained until GABAergic commissures analysis. Scoring was performed in 0.5-1 h post-hatching (early L1 larva) and L4 animals (green arrows). A two-tailed unpaired Student's t-test was used for statistical analysis. Data represent three independent trials with at least 20 worms per trial. Results are presented as mean ± SD.

References

1 Blanco, M. G. *et al.* Diisopropylphenyl-imidazole (DII): A new compound that exerts anthelmintic activity through novel molecular mechanisms. *PLoS Negl Trop Dis* **12**, e0007021, doi:10.1371/journal.pntd.0007021 (2018).

2 Donnelly, J. L. *et al.* Monoaminergic orchestration of motor programs in a complex C. elegans behavior. *PLoS. Biol* **11**, e1001529, doi:10.1371/journal.pbio.1001529 [doi];PBIOLOGY-D-12-03108 [pii] (2013).

3 Oliver, D. *et al.* Integrins Have Cell-Type-Specific Roles in the Development of Motor Neuron Connectivity. *J Dev Biol* **7**, doi:10.3390/jdb7030017 (2019).

4 De Rosa, M. J. *et al.* The flight response impairs cytoprotective mechanisms by activating the insulin pathway. *Nature* **573**, 135-138, doi:10.1038/s41586-019-1524-5 (2019).

5 Andersen, N. *et al.* 1-Mesityl-3-(3-Sulfonatopropyl) Imidazolium Protects Against Oxidative Stress and Delays Proteotoxicity in C. elegans. *Front Pharmacol* **13**, 908696, doi:10.3389/fphar.2022.908696 (2022).

6 Belew, M. Y., Huang, W., Florman, J. T., Alkema, M. J. & Byrne, A. B. PARP knockdown promotes synapse reformation after axon injury. *bioRxiv*, doi:10.1101/2023.11.03.565562 (2023).

7 Gujar, M. R., Stricker, A. M. & Lundquist, E. A. Flavin monooxygenases regulate Caenorhabditis elegans axon guidance and growth cone protrusion with UNC-6/Netrin signaling and Rac GTPases. *PLoS Genet* **13**, e1006998, doi:10.1371/journal.pgen.1006998 (2017).